

Master's Thesis

Design and Implementation of Acoustic Phased Array for In-Air Presence Detection

Addythia Saphala

University of Freiburg

Faculty of Engineering

Department of Microsystems Engineering - IMTEK

Laboratory for Electrical Instrumentation

July 24th, 2019

Writing Period

24. 07. 2018 – 24. 07. 2019

Examiner

Prof. Dr. Leonhard Reindl

Second Examiner

Prof. Dr. Christian Schindelhauer

Advisers

M. Sc. Dominik Jan Schott

Declaration

I hereby declare, that I am the sole author and composer of my thesis and that no other sources or learning aids, other than those listed, have been used. Furthermore, I declare that I have acknowledged the work of others by providing detailed references of said work.

I hereby also declare, that my Thesis has not been prepared for another examination or assignment, either wholly or excerpts thereof.

Freiburg, 24.07.2019

Addythia Saphala

Abstract

In this work a device for utilizing acoustic signal reflection for presence detection is realized. The system consists of a transmitter and a synchronized phased array receiver to derive the position of the objects from which the transmitted signal is reflected. This device serves as a prototype to investigate a suitable arrangement for presence detection by echolocation in an enclosed space. The hardware design and construction, system overview, and underlying principles to detect and locate objects are explained in the Chapter 4. Furthermore hardware validation, calibration and visualization of the result are detailed in the Chapter 5. The device is used in a ceiling-mounted configuration, with four elements microphone array, arranged in a square which are equidistant from the speaker. The presence detection methods used for this arrangement are detailed in this work.

Contents

Abstract	iii
1. Introduction	1
2. Related Work	3
2.1. State-of-the-art	3
2.2. Literature Review	4
2.3. Chapter Summary	6
3. Background	7
3.1. Acoustics	7
3.1.1. Acoustic wave	7
3.1.2. Speed of sound	7
3.1.3. Chirp	8
3.1.4. Window	9
3.1.5. Acoustic Source	9
3.1.6. Reflection	10
3.1.7. Reverberation	10
3.1.8. Echolocation	10
3.1.9. Phase Array	11
3.2. Electronics and Hardware	12
3.2.1. Sensor	12
3.2.2. Transducers	13

3.2.3. Active Filters	13
3.2.4. ADC and DAC	14
3.2.5. Microcontroller	14
3.2.6. PC-Server host	15
3.2.7. Power Supply Unit	15
3.2.8. Experiment Equipment	15
3.3. Analog Signals	16
3.3.1. Single ended vs balanced signal	16
3.3.2. High-Pass Filter	16
3.3.3. Band-Pass Filter	17
3.3.4. Instrumentation Amplifier	18
3.3.5. Non-Inverting Amplifier	18
3.4. Digital Signal Processing	19
4. Approach	21
4.1. System Overview	21
4.1.1. Hardware	23
4.1.2. Software	33
4.1.3. Room Setup	35
4.2. Calibration	38
4.2.1. Speed of Sound	38
4.2.2. Inter-channel Delay	38
4.3. Chirp Selection	39
4.4. Presence Detection	39
4.4.1. Empty Room Echo Profile	39
4.4.2. Peak Selection	39
4.4.3. Distance Map	42
4.4.4. Direct Intersections	43
4.4.5. Sonogram	43
4.4.6. Angle of Arrival and Time of Flight Estimation	43

4.5.	Retired Configuration	49
4.5.1.	Control	49
4.5.2.	Transmitter	51
5.	Experiments	53
5.1.	Hardware Validation	53
5.1.1.	Speaker and Microphones	53
5.1.2.	Pre-Amplifiers	55
5.1.3.	Active Filters	58
5.1.4.	ADC	58
5.1.5.	Concluding Remarks	58
5.2.	Device Calibration	60
5.2.1.	Inter-channel Delay	65
5.2.2.	Speed of Sound	66
5.2.3.	Concluding Remarks	66
5.3.	Chirps	66
5.3.1.	Concluding Remarks	69
5.4.	Presence Detection	69
5.4.1.	Static Object	70
5.4.2.	Helmet vs Head Reflection	73
5.4.3.	Elementary Tracking	76
6.	Discussion and Conclusion	77
6.1.	Hardware Evaluation	77
6.1.1.	Transmitter	77
6.1.2.	Receiver	77
6.2.	Software Evaluation	78
6.2.1.	Transmitter	78
6.2.2.	Receiver	78
6.3.	Digital Signal Processing	79

6.4. Localization	79
6.5. Conclusion	80
6.6. Future Outlook	81
6.7. Recommendation for Hardware Development	82
6.8. Recommendation for Software Development	82
6.9. Recommendation for Localization and Tracking	83
7. Acknowledgments	85
A. Appendix	87
A.1. Schematics	87
Bibliography	99

List of Figures

3.1. Acoustic Wave	8
3.2. Simplified Bat Echolocation	11
3.3. Bat Echolocation Timeline	11
3.4. Phase Array	12
3.5. Single-ended vs Balanced Signal	16
3.6. High-Pass Filter	16
3.7. Band-Pass Filter	17
3.8. Instrumentation Amplifier	18
3.9. Non-Inverting Amplifier	18
4.1. Hardware Overview	22
4.2. Hardware Configuration	24
4.3. Microphone Overview	25
4.4. Receiver PCB	26
4.5. Receiver Filter Stages	27
4.6. Receiver Active Filter	27
4.7. Transmitter	30
4.8. External Amplifier	31
4.9. Power Supply	32
4.10. Plate Holder	32
4.11. Transmitter Flowchart	33
4.12. Receiver Flowchart	34

4.13. DSP Flowchart	36
4.14. Experiment Room	37
4.15. Echo Profiles	40
4.16. Static Object	41
4.17. Direct Intersection	44
4.18. Sonogram	45
4.19. Octant Division	46
4.20. Wave front Azimuth	47
4.21. Azimuth	48
4.22. Retired Control	49
4.23. Retired Transmitter	51
5.1. Hardware Validation	54
5.2. Frequency Response of Speaker vs Reference Microphone	55
5.3. Frequency Responses	56
5.4. Setup for Sine Sweep Test	56
5.5. Pre-Amplifier	57
5.6. Pre-Amplifier	59
5.7. ADC Validation Setup	60
5.8. Channel Test	61
5.9. Measured Signal and Digital Readout	62
5.10. ADC Amplitude Spectrum	63
5.11. Device Calibration	64
5.12. Chirp Selection Experiment	67
5.13. Chirp Selection Result	68
5.14. Experiment Setup	69
5.15. Experiment Setup	70
5.16. Direct Intersection Results	72
5.17. Direct Intersection Results	74
5.18. Head vs Helmet	75

List of Tables

3.1. Microcontroller Comparison	14
4.1. ADS8588s Pin Map	29
4.2. Retired Control Pin Connection	50
5.1. Calibration Result	60
5.2. Measured Distances	71
5.3. Calculated Coordinates	71
5.4. Direct Intersection Coordinates	72
5.5. AoA and ToF Spherical Coordinates	73

1. Introduction

Presence detection is a topic of interest with variety of application. Recent trends in technologies within the last decades and the rise of Internet-of-Things leads to development of various “smart” devices [1, 2]. Information about the presence of persons or objects inside a room can serve multiple functions such as security, energy conservation, and occupancy detection [3, 4, 5]. In this work, a device for detecting presence via acoustic echolocation is realized. After transmitting an acoustic signal, each microphone records the returning echoes to determine the location of reflecting object. The location can then be derived by using a phased array set-up and calculating the delay between echoes [6].

Echolocation is used in nature by a wide variety of bats to navigate and detect objects [7]. The focus of this work is to utilize this phenomenon for presence detection of people inside enclosed rooms. Furthermore, micro speakers (speakers for small devices) and MEMS microphones are used to realize a low cost and functional device. As a preliminary work for further research, several assumption is made for the starting point of the experiment. The room for the experiment is enclosed and without any wind current. Therefore the assumption is that the air as the medium of the acoustic wave is homogeneous and isotropic. Moreover the object of detection is also assumed to have smooth surface with normal vector toward the device and sufficient reflecting coefficient for acoustic wave [8].

The device is developed as a prototype for detecting presence via echolocation.

Echolocation is used in this work because it has excellent properties to detect solid surfaces relatively independent of light and radio frequency [8]. Therefore it can also be used as part of sensor fusion for object detection to increase the reliability of the overall detection system. Moreover since acoustic signals beyond hearing range in air is less disruptive, it can be used in normal environments e.g. office, home and public spaces [9].

Works relevant to this thesis are reviewed in Chapter 2, including commercially available devices and state-of-the-art. Background theories and several key points used throughout this work are described in Chapter 3. Chapter 4 describe the problems and approach of this work, including the system overview and room setup. The experiment and result are presented in Chapter 5, with the conclusion in Chapter 6.

It is the author's hope that this thesis can be used as one of the foundation work for future research in this topic.

2. Related Work

According to educational resources from IEEE Ultrasonics, Ferroelectrics and Frequency Control Society, ultrasonic sensor in air is divided into several classifications. This work would be classified as an Ultrasonic distance sensor, since it detects echoes and derive results from reflected signals [10]. Topics relevant to this will be further discussed in this chapter. Starting with available state-of-the-art systems that utilize acoustic signal as means of presence detection in Section 2.1. Followed by the literature review of related works in Section 2.2 and concluding remarks in Section 2.3.

2.1. State-of-the-art

One of the most common ultrasonic sensor that can be used for presence detection available right now is a simple ping sensor e.g. HC-SR04 and Maxbotix LV-MaxSonar sensor series. In this type of sensors measure the time of flight from reflected acoustic signal and time of transmission. These sensors generally has very high directivity and narrow field of view. To utilize these sensors as presence detector, strategic placement and static area of detection are required [11, 12]. Furthermore multiple sensors are required to cover a large area and visible installation within reach e.g. on the desk or chair can be inconvenient. To avoid cross-interference between multiple sensors due to transmission from a sensor transmitter to a receiver on a different sensor, a transmission slot allocation is also required [13].

Toposense, a company based in Munich, has developed sensors for ultrasonic echolocation. One of their latest TS series device, TS-3 is intended for close range perception in autonomous robots. This device has 160 by 160 degree field of view and scan ranges up to 5 meters [14, 15, 16].

Steinel, a company founded in Rheda-Wiedenbrück also sells several type of ultrasonic based presence detectors. Their devices are intended for building automatons. Most of Steinel's ultrasonic sensors are installed on the ceilings or walls and provide static points of detection for a single room.

Telocate ASSIST, a system developed by Telocate is an active ultrasonic location detection system. A transmitting tag is attached to objects of detection and monitored by a sensor array mounted on the ceiling. The location of the tag is then derived from the time delay between received signals.

INFsoft also offers similar systems using various technologies such as Bluetooth, Wi-Fi, ultrasound, RFID and ultrawideband for indoor navigation, localization and tracking.

Elliptic labs from Oslo, Norway develop software only for ultrasound presence sensing either by using smartphones or any devices with speakers and microphones. This system, called Inner Reflection only detect presences within certain range from the devices.

2.2. Literature Review

There are various method of presence detection with acoustic signal. Active detection by using transmitter attached to the object or passive detection by capturing the reflected signals. Simple detection scheme with array of ping sensor, as well as transceiver pair to detect presence by disturbances. In this work we concern our-self mainly with passive means of presence detection, that is we use a single transmitter -

as acoustic wave source, and capture the echoes from the objects with phased array. In this section we review several work that utilize similar concept to detect presence inside enclosed room.

David Caicedo and Ashish Pandharipande presented an ultrasonic sensor for localized presence sensing by using single transmitter and a linear array. This device was used for several different experiments. By mounting the device on the ceiling facing downward, this device can detect and track presence in different tracking zone based on difference of arrival angle [17]. For localized presence sensing, the device was installed vertically in a manner that the array of microphones were placed horizontally at the height of detection zone. The location and movement of the presence can be derived from the angle of arrival of reflected signal [18]. The application of multiple sensors to form an sensor array to improve spatial coverage were also considered. By time gating the time of detection multiple sensor can be used to cover more space [13, 5].

Naghizadeh *et al.* presented an ultrasonic circular array sensor for granular presence sensing. Granular means that it have a degree of position detection of the presence. The array of eight microphone were arranged in circular fashion, with single transmitter. This sensor was intended for ceiling mounted configuration. The sensor were able to detect and track presence in the test office location by deriving the range, azimuth and elevation from reflected signal [19, 20].

Ribeiro *et al.* were able to obtained room models by using a compact array of microphones. The transmitter is co-located with receiver array, therefore by emitting known test signal the room impulse responses can be estimated. The device used in this experiment was a low-cost off the shelf teleconferencing device [21].

Patent US8844361 describe an invention of ultrasonic sensor control system for occupancy sensing. This invention consist of ultrasonic transmitter with amplitude control to adjust area of detection. The principle of detection is also based on

echolocation, where people inside area of detection would reflect signal into the receiver [22].

The devices and systems work based on principles of echolocation. By using an array of receiver, the angle of arrival of the reflected signal can be derived. If the transmission time is also known, then the range can be calculated by multiplying speed of sound with the time delay between transmission time and received time. The configuration of receivers are fixed in both devices, in our work the configuration of microphone array are designed to be flexible and can be reconfigured as necessary.

2.3. Chapter Summary

The review of several available systems and publications as shown above can be summarized as follows: While there are a variety of methods to detect presences via ultrasound, in this thesis we focus on echolocation methods. As we wish for low-cost and flexibility, our design is limited to off the shelf component, which limits our bandwidth and signal capabilities. Caicedo and Naghibzadeh showed various arrangement of device configurations for presence detection and Ribeiro showed that solid surfaces can be detected with off the shelf consumer product hardware. As there are few comparable systems available for indoor echolocation, therefore active SONAR approaches for indoor detection of objects are investigated.

3. Background

In this chapter, the terms and concept used in this thesis are explained. The basics include acoustics in Section 3.1, electronics in Section 3.2 and digital signal processing in Section 3.4.

3.1. Acoustics

3.1.1. Acoustic wave

The term acoustic wave in this work refers to fluctuation of pressure within compressible fluid or air. The sequence of compression and rarefaction wave that travel through the medium in audible frequency range can be perceived as sound. On higher or lower frequency as ultrasonic or infrasonic wave they are beyond the hearing limit, approximately from 20 Hz to 20 kHz. The adjacent region of compression and rarefaction produced by the individual element movement within the fluid in the direction of the forces, similar to longitudinal waves in a bar [8].

3.1.2. Speed of sound

The speed of sound propagation through fluid is one of important parameter in this work. Kinsler *et al.* [8] derived the theoretical speed of sound in air at 0°C and 1

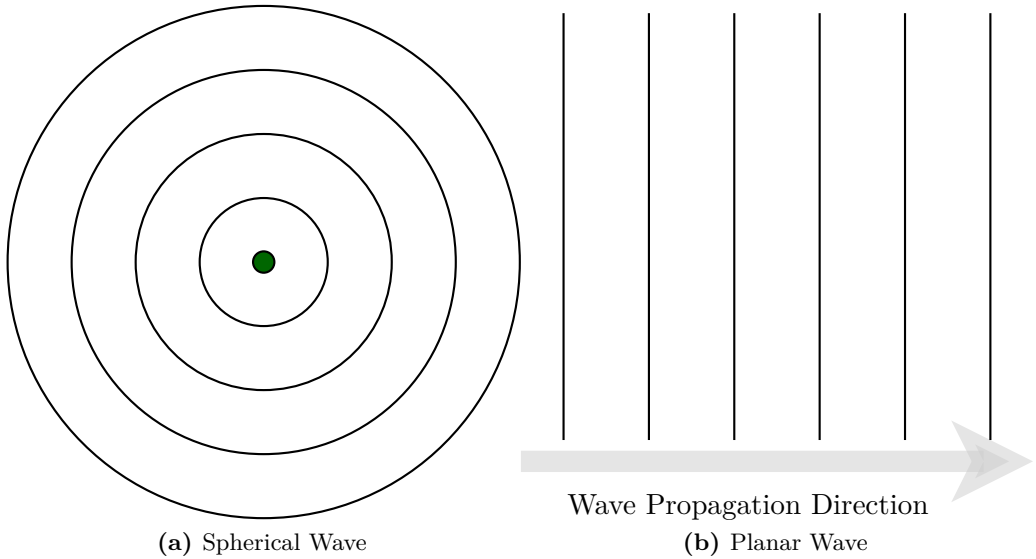


Figure 3.1.: Acoustic Wave

atm pressure as:

$$c_0 = 331.5 \text{ m s}^{-1} \quad (3.1)$$

and the speed of sound is proportional to the square root of the absolute temperature:

$$c = c_0(1 + T/273)^{1/2} \quad (3.2)$$

These theoretical values and equation are derived for adiabatic condition, where the sound wave propagate through perfect gas. Although the condition in real environment might not completely ideal due to air current and mixture of gasses, for the scope of this work the speed of sound indoor is assumed to be constant.

3.1.3. Chirp

Chirp signal is a frequency modulated signal. In nature, bats utilize this frequency-modulated signal for echolocation [7]. While a chirp signal has various parameters, within the scope of this work the signals are limited to linear up-chirps. Linear up-

chirps refer to the instantaneous frequency of the signals which increase linearly with time. Chirp signals or sine sweep signals can be utilized for the measuring impulse response and transfer function of devices [23, 24].

3.1.4. Window

To avoid sharp amplitude transition and resulting clicking artifacts from the speaker, a window has to be applied to the signal. For the purpose of this work, a simple raised cosine window is used. Similar to Chan [24] who used fade-in/out window, the signal is multiplied with the window of the same length.

3.1.5. Acoustic Source

In this work, the acoustic wave source is simplified into a point source since the radius of the source is small compared to the wavelength. With the assumption that the fluid media is isotropic and homogeneous, the acoustic wave can be approximated as a spherical waves. This point source then can be simulated as a pulsating sphere source, referred as simple source [8]. A simple source will emit spherical acoustic field independent of their shapes, given that the source have the same volume velocity and the wavelength is greater than the dimension of the source [8]. At a distance more than several wavelength from the source, the spherical wave can be approximated as a plane wave. However the pressure amplitude of spherical wave decrease inversely with the distance while plane wave pressure amplitude stays constant [8]. The equation for outgoing spherical wave is:

$$p(r, t) = (A/r)e^j(\omega t - kr) \quad (3.3)$$

Therefore, the pressure is inversely proportional with an exponent of the distance, depends on the frequency [8].

3.1.6. Reflection

When the acoustic wave encounters a change in acoustic impedance of the wave is passing through the medium and some of it is reflected back. For perpendicular or normal incidence the reflection direction is the opposite of transmission direction, else the incidence angle is mirrored to the reflection angle. In this thesis, the main focus of this phenomenon is when the sound wave encounter solid objects. With the assumption that the wave arrive at normal incidence [8].

3.1.7. Reverberation

Architectural reverberation happens in an enclosed room is proportional to its size and amount of sound absorbing material present in the room. Due to the sound travels outwards in diverge manner, waves are partially absorbed and reflected due to the boundary of the room. A new sound can be masked due to interference from this reverberant sound and prevent immediate recognition until sufficient time has elapsed [8].

3.1.8. Echolocation

Echolocation, such as the method used by bats to locate their prey, is a phenomenon where the reflected sound waves are used to determine the location of objects or surfaces which reflect the sound waves. This concept has been extensively used for various research and development in engineering, such as sound navigation and ranging (SONAR) [25]. For bats, the incoming reflected waves direction can be resolved due to complex signal processing in the bat's ears and brain. While bats' echolocation system is not completely understood, one of the more obvious parts is the time difference of arrival between left and right ear, which can be used to calculate the incoming sound wave direction [26]. Figure 3.3 shows the transmit

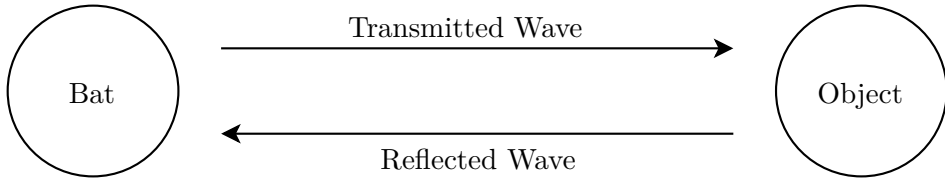


Figure 3.2.: Simplified Bat Echolocation

time t_0 , the time reflected sound wave arrived in one ear t_1 and in the other ear t_2 . The difference between t_1 and t_2 can be used to derive the angle of arrival, and the difference of both of them to t_0 can be used to calculate the range.

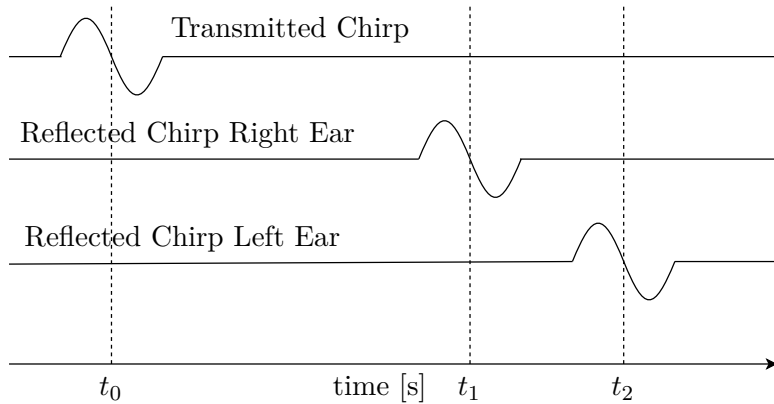


Figure 3.3.: Bat Echolocation Timeline

3.1.9. Phase Array

Phase arrays are used to determine the angle of arrival of incoming acoustic wave [8].

In Figure 3.4, the elevation, θ is calculated as:

$$\theta = \arccos\left(\frac{d}{r}\right) \quad (3.4)$$

$$d = c \cdot \Delta t \quad (3.5)$$

Where d is the product of speed of sound and the time difference of arrival, while r is the distance between microphones.

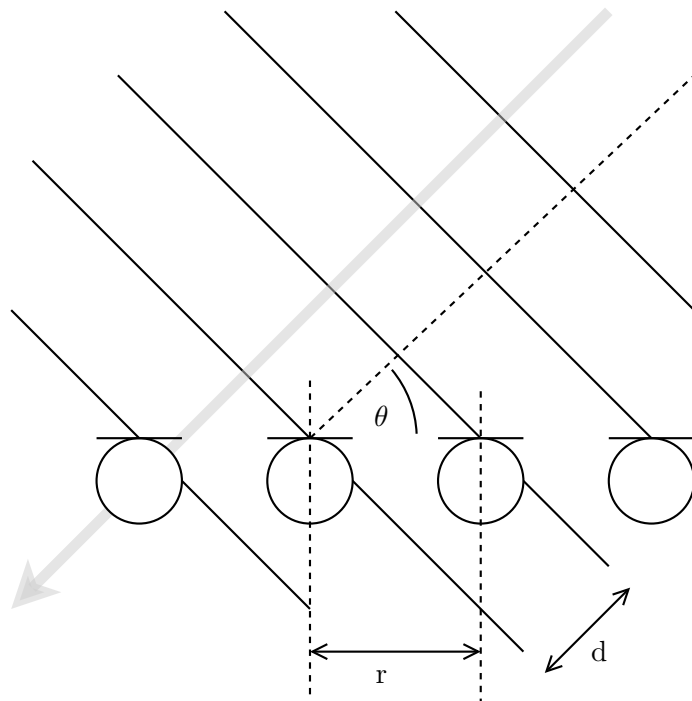


Figure 3.4.: Phase Array

3.2. Electronics and Hardware

3.2.1. Sensor

Sensors are defined as devices that detect physical phenomenon and transmit signals to send information to other electronic devices in the system. The sensor in this thesis is developed for presence detection and providing location information of objects. The design and construction of this sensor is discussed further in Chapter 4. The term "Active Sensor", "Active SONAR", and "Passive Localization System" are applicable to the device developed here. Active sensors emit energy into the system and derive information from the emitted or reflected energy, or both. Passive sensors derive the information of the environment based on received energy alone, without transmitting any energy into the system [27]. Active SONAR is defined as SONAR systems based on reflected acoustic wave by target objects, while passive is SONAR

defined as SONAR system based on passively listening on acoustic wave emitted by target objects [8]. Active and passive localization system differ based on whether the system using active sender or tag to mark the location or object. Active localization system use tags or devices to track and detect objects, while passive localization system does not use any such tags or devices [28].

3.2.2. Transducers

A transducer is a component that is used to convert one type of energy to another. Within the scope of this work only in air electro-acoustic transducers are used, in particular MEMS Microphones and micro speakers. Microphones are component or device that convert acoustic waves into electrical signals, while speakers are device that convert electrical signals into acoustic waves [8], The MEMS Microphone used, ICS-40720 [29], is a differential output MEMS Microphone. This microphone has an extended frequency response up to 20 kHz, good signal to noise ratio (70 dBA) and omni-directionality. It has the flexibility to have a balanced output or a single ended output. This microphone is also recommended for microphone array applications [29]. The speaker used is AS01508AO [30] from PUI Audio. The speaker is a slim-line micro speakers intended for space-limited modern electronics. The speaker size is 15mm x 11mm, with 0.7 W continuous power and 1 W maximum power. The characterization of this speaker from Zeqiri [31] at 16, 18, 20, and 22 kHz shows excellent directivity.

3.2.3. Active Filters

An active filter is a combination of passive filter components with active components. The active components commonly used are amplifiers. Active high pass filter and active band pass filter can be created from a combination of passive RC filter network and an operational amplifier. The filters and microphone pre-amps are described

in Chapter 4. The op-amp used in the active filters for pre amp and receivers are OPA1654 and OPA1652. While OPA1632, and TPA6205A are used in the retired multi-channels transmitter more details of retired parts are in Section 4.5. These amplifiers are chosen for their high signal to noise ratio, high linearity at higher frequency and partially based on previous work in Telocate ASSIST.

3.2.4. ADC and DAC

Analog to Digital Converter (ADC) and Digital to Analog Converter (DAC) are used in the receiver and transmitter respectively. These components are used to do a conversion between analog and digital domain. The ADC used in the receiver is ADS8588S, it has eight channels, 16 bit resolution and simultaneous sampling. The DAC used in the retired transmitter is PCM1690, while the the transmitter used in this work is the SGTL5000 audio chip.

3.2.5. Microcontroller

Microcontroller is an electronic component or devices which utilize microprocessor to act as a control device. Table 3.1 shows the considered parameters for microcontroller selection. The RAM is important for buffering the signal, while high clock speed is required for reasonable transmitting time.

Table 3.1.: Microcontroller Comparison

Microcontroller	Microprocessor	RAM	Clock
Arduino Mega 2560	ATmega2560	8 KB	16 MHz
Arduino Due	AT91SAM3X8E	96 KB	84 MHz
Arduino MKR Zero	Cortex-M0 + ARM MCU	32 KB	48 MHz
Teensy 3.6	Cortex-M4F + MK66FX1M0	256 KB	180 MHz

3.2.6. PC-Server host

In this stage of development, for ease of development the digital signal processing was done in MATLAB. For real-time application, computers used as the server is Intel NUC7i5DKNE, and MSI GS70.

3.2.7. Power Supply Unit

The power supply unit (PSU) used in this work needs to be able to supply +5 V, -5 V, and ground connection. The power circuit converts 12 V from battery into a balanced output with low noise for audio applications. This output connected to power hub circuit via banana jacks, then from power hub circuit into receiver and the microphone via molex 3-pin connectors. The cable from circuit hub to the microphone has to be twisted to reduce noise.

3.2.8. Experiment Equipment

- **Anechoic Chamber** For hardware validation and calibration an anechoic chamber is used to provide controlled environment. The box measurement is 1m x .5m x .5m, lined with sound absorbent materials inside. The anechoic box is shown in Figure 5.1.
- **Audio Interface** The audio interface used as tools for hardware validation is Focusrite Scarlett 18i20 2nd Gen.
- **Reference Microphone** The reference microphone for hardware validation is Earthworks M50.
- **Laboratory Power Supply** The power supply used for validation and calibration is Protek Dual DC Power Supply 3032B.

3.3. Analog Signals

3.3.1. Single ended vs balanced signal

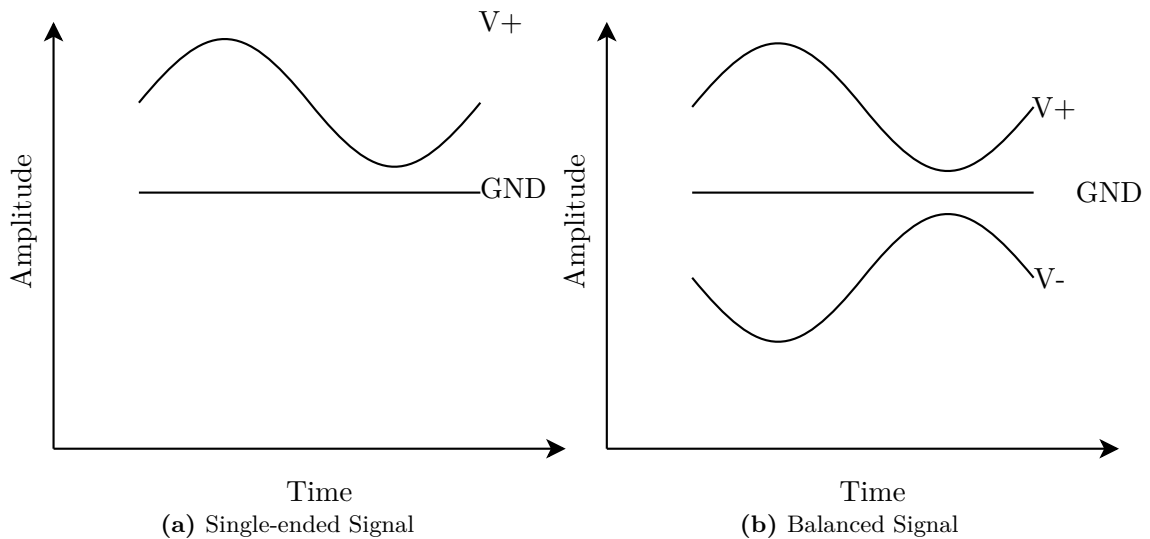


Figure 3.5.: Single-ended vs Balanced Signal

Figure 3.5 shows the difference between a single ended signal and a balanced signal. Balanced signals have the advantage of being resistant against common mode noise, which is the reason why it is favored for long distance connections.

3.3.2. High-Pass Filter

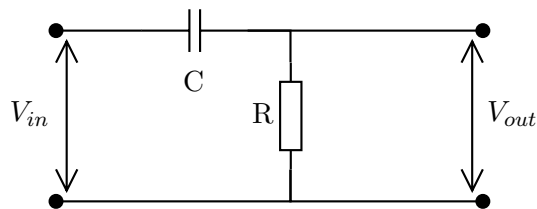


Figure 3.6.: High-Pass Filter

A High-Pass Filter is a passive electronic RC circuit used for attenuating lower

frequency signals. The equation for the cut off frequency of a high pass filter:

$$f_c = \frac{1}{2\pi RC} \quad (3.6)$$

3.3.3. Band-Pass Filter

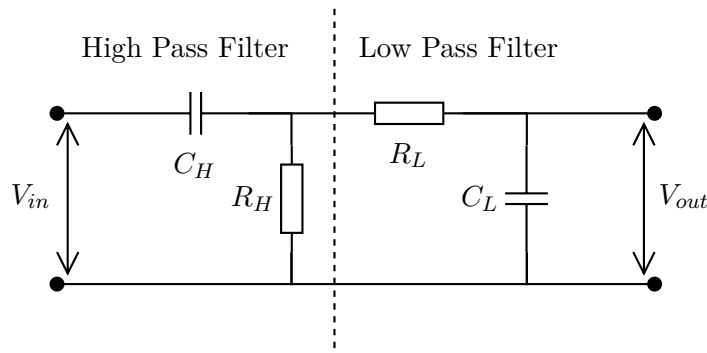


Figure 3.7.: Band-Pass Filter

A band-Pass filter can be build by a combination of low pass and high pass filters, to only allow signal within certain frequency range to pass through. The equations for the cut off frequencies is simply the cut off frequency for the high pass filter for the lower limit, f_L , and the low pass filter for the higher limit, f_H .

$$f_L = \frac{1}{2\pi R_H C_H} \quad (3.7)$$

$$f_H = \frac{1}{2\pi R_L C_L} \quad (3.8)$$

$$f_r = \sqrt{f_L \cdot f_H} \quad (3.9)$$

R_H and C_H are resistance and capacitance of the high pass filter part, while R_L and C_L are from the low pass filter part. f_r is the central resonant frequency.

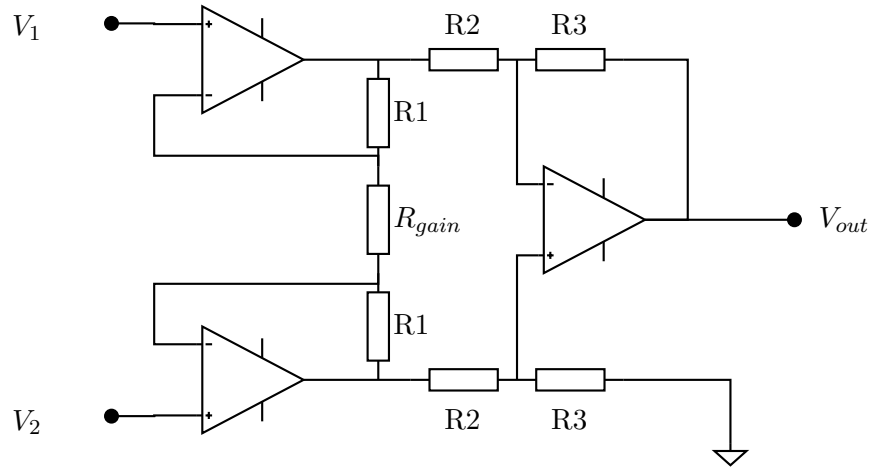


Figure 3.8.: Instrumentation Amplifier

3.3.4. Instrumentation Amplifier

$$A_v = \frac{V_{out}}{V_1 - V_2} = \left(1 + \frac{2R_1}{R_{gain}}\right) \frac{R_3}{R_2} \quad (3.10)$$

An instrumentation amplifier is used for amplification of balanced signals and convert the signals into a single ended output. Equation for gain of an instrumentation amplifier. In the case where $R_3 = R_2$, then the gain would be:

$$A_v = 1 + \frac{2R_1}{R_{gain}} \quad (3.11)$$

3.3.5. Non-Inverting Amplifier

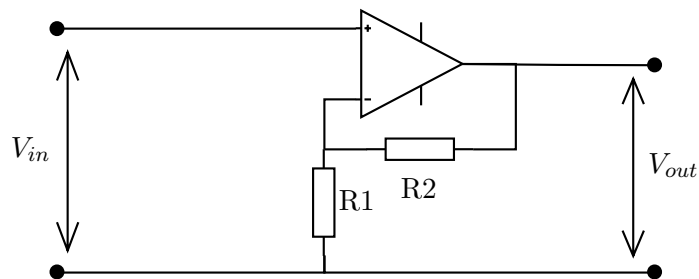


Figure 3.9.: Non-Inverting Amplifier

A non-inverting amplifier is used to amplify signals without reversing the polarity. Equation for the gain of non-inverting amplifier is:

$$A_v = \frac{V_{out}}{V_{in}} = 1 + \frac{R_2}{R_1} \quad (3.12)$$

3.4. Digital Signal Processing

In this section, the signal processing used in this work are shortly mentioned. From analog to digital domain signal conversion, there are several consideration needed. The sampling frequency is the number that shows how often the analog signal is sampled. The Nyquist criterion states that for sinusoidal signal, the signal have to be sampled at least twice of the signal frequency [32]. This is true for both ADC and DAC operations. The maximum sampling frequency for the receiver is 50 kHz and the maximum sampling frequency of the transmitter is 44.1 kHz, which means the maximum frequency of the signal is 22.05 kHz.

Matched filters are usually used to determine time delay estimation of waveforms. In the simplified form, the purpose of matched filter is to find a measure of similarities between two sequences. For this purpose we can use a mathematical equation known as cross-correlation [33]. Cross-correlation function (ccf) result in a peak, where the signals that are in phase have similar frequency content.

Interpolation are used for expanding sample number by estimating the value of interpolated point in between measured sample. Zero Padding Interpolation add zero padding in frequency domain to exploit the fact that by adding zeros in the middle of the function, the frequency result shifted up throughout the sequences, which in effect increasing the number of sample while keeping the signal form. This only hold true if the signal is sinusoidal [34]. Fourier transform is the mathematical operation to view the signal in frequency domain. The Fast Fourier Transform (FFT) is a

faster way to compute Discrete Fourier Transform (DFT) [35]. We use this function in this work to calculate the frequency domain of signals.

Envelope function is used when the outer limit of signal sequence is of interest. For causal and real signal, the absolute value of hilbert transform can be used for this purpose. The result of this hilbert function is an analytic signals, which is a complex signals which has no negative frequency components [36].

Local maxima in a signal refer to peak in the sequence. In the result of cross-correlation, a peak mean that there is a degree of similarities to signals in that phase with the correlating signal [37].

4. Approach

In this chapter, several problems and the experimental approaches to solve it are described. In progress of this work, the hardware verification and validation of the approach went through several iterations. The system overview covers the hardware constructions and designs. The experimental nature of this work began with series of preliminary research to consider the viability of the overarching concept of the device. Followed by the designing phase of the device, then debugging and characterization. After the device is ready, we started to iterate several possible parameters to figure out the viable parameters, such as chirp parameters, overall digital signal processing parameters and channels calibration. In the validation and calibration phase, we utilize anechoic box to verify whether line of sight and channels calibration are sufficient. First, the frequency response and the channel characteristic are derived from the line of sight calibration with a sine sweep signal. Then the calibration for delay within the channels and the speed of sound at the time of the experiment can be calculated. After that we consider several chirp signals to be selected for the experiment. Finally, in the experiment phase, the device is mounted above objects of detection, facing downward similar to ceiling mounted devices.

4.1. System Overview

Figure 4.1 present the simplified hardware overview. The system used a single speaker and an array of microphone inside the experiment room. An external amplifier is

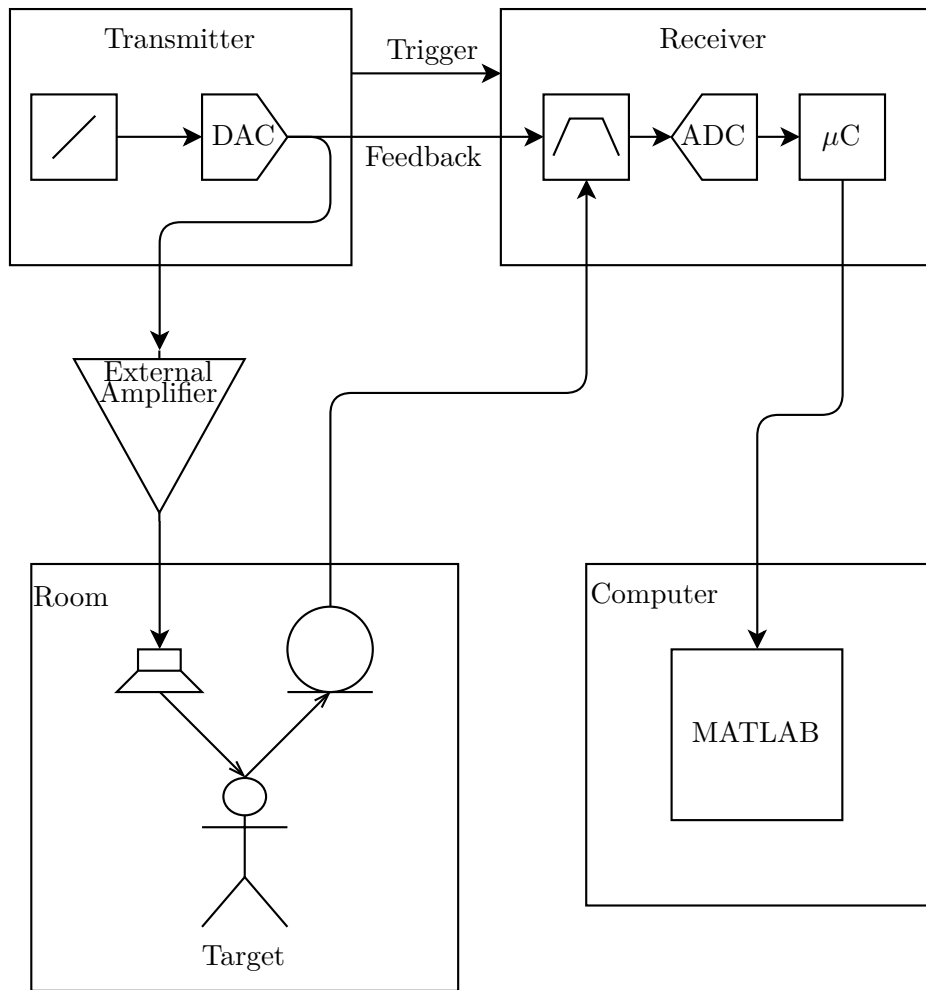


Figure 4.1.: Hardware Overview

needed to boost the volume of acoustic signals since the working frequencies is far from optimal the speaker frequency response. The transmitter sends a trigger signals into the receiver as the audio playback starts to start the recording function. The recorded signals contain the line of sight (direct) waves as well as reflected (echo) waves. The entire recorded signals is henceforth referred as a "frame". This frame is transmitted into the computer via USB connection. The digital signal processing then takes place in MATLAB environment.

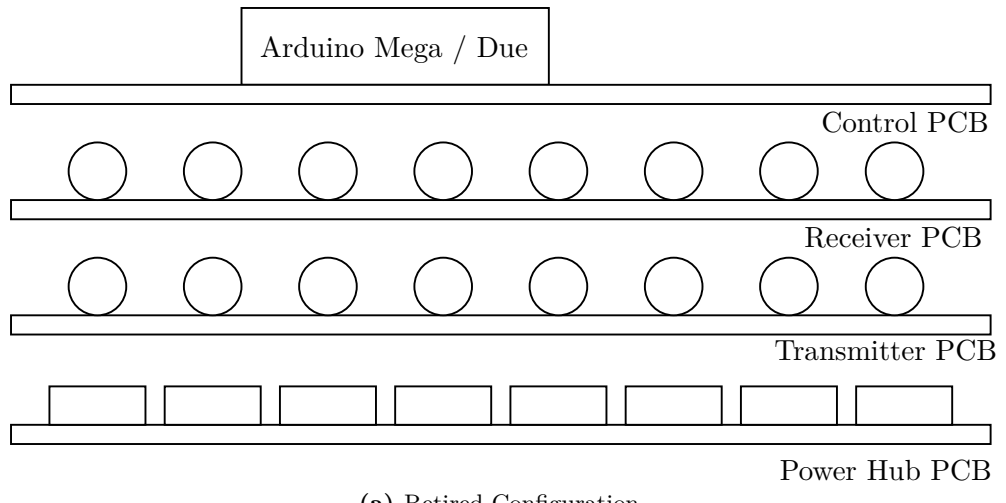
4.1.1. Hardware

Figure 4.2 shows the flexible stacked configuration of the old (retired) and new (working) hardware configuration. In the retired configuration, eight channel transmitter and receiver are attempted. This approach is shelved for this work and the new configuration is used instead. Section 4.5 provides more information of the hardware used in retired configuration. The working configuration provides eight channel receiver and a separate single channel transmitter. Picture of the device configuration can be found in appendix.

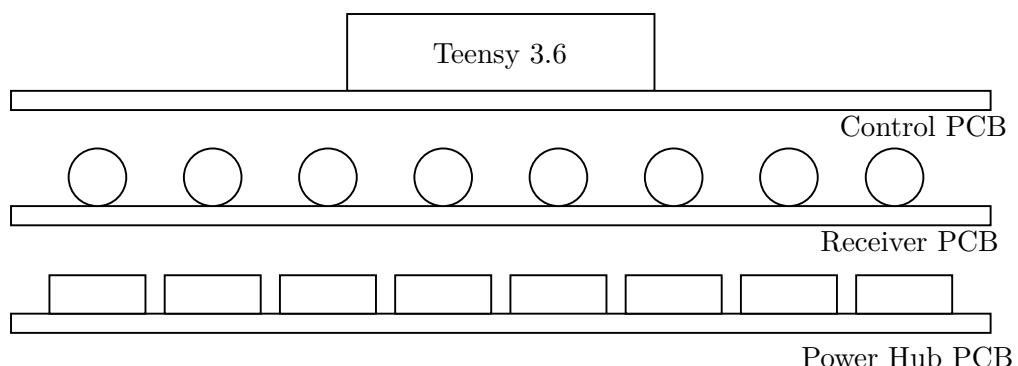
Microphone

Figure 4.3 shows the design and construction of the microphone. This device composed of a MEMS Microphone ICS-40720 and active filter with op-amp OPA1652. The power part of the circuit is used to supply 3.3V for the MEMS microphone, the power supply from the power hub consist of +5V, -5V and ground connection which directly supply the amplifier. The filter is a high pass filter RC circuit intended to filter out power coupled noise. The cut off calculated from equation Equation (3.6).

$$f_c = \frac{1}{2\pi \cdot 10 \text{ k}\Omega} \cdot 1 \text{ nF} = 1.59 \text{ kHz} \quad (4.1)$$

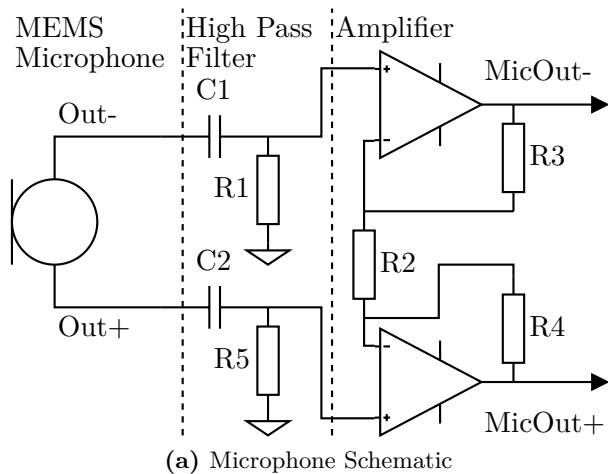


(a) Retired Configuration

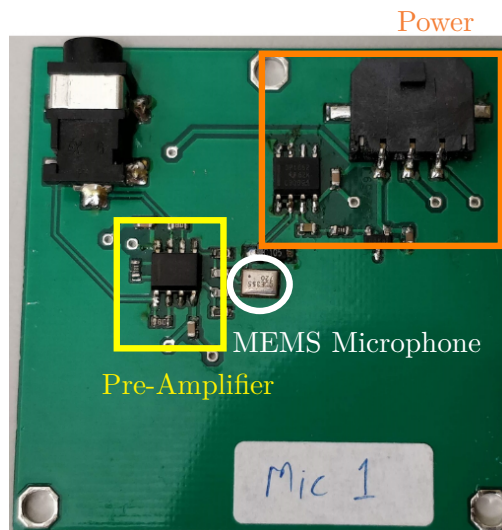


(b) Working Configuration

Figure 4.2.: Hardware Configuration The device has a layered configuration, circles indicate audio jack connections and the square on the power hub PCB indicate power connectors.



(a) Microphone Schematic



(b) Microphone Picture

Figure 4.3.: Microphone Overview

The amplifier is the first half of an instrumentation amplifier. Since the later half is an unity gain differential amplifier, from Equation (3.11) the gain can be calculated as:

$$A_v = 1 + \frac{2 \cdot 1 \text{ k}\Omega}{180 \Omega} = 12.11 \text{ V/V} \quad (4.2)$$

The device depicted in Figure 4.3 henceforth referred as microphone.

Receiver

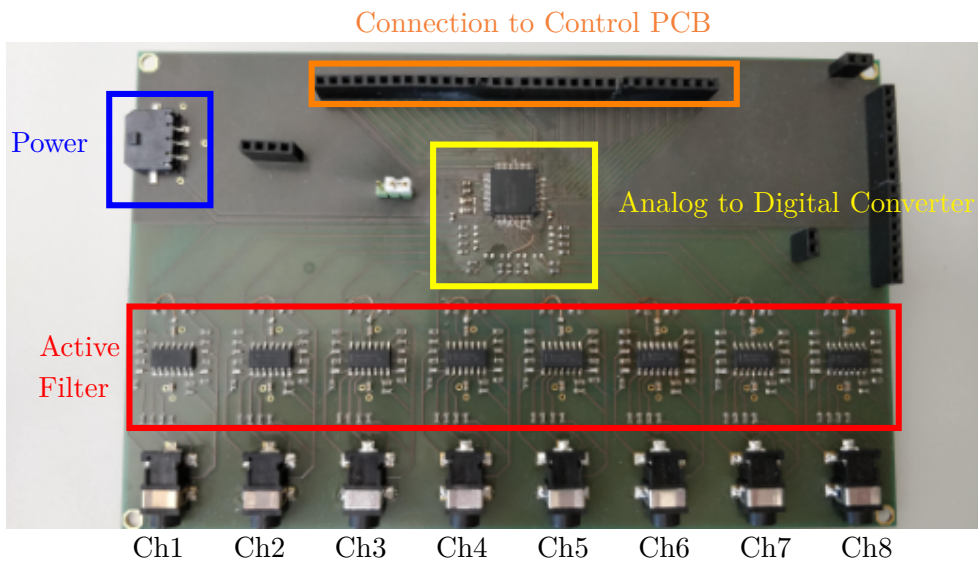


Figure 4.4.: Receiver PCB

Figure 4.4 shows the eight channels receiver PCB. The signal path is from input jack through active filter to the ADC. The ADC then transmit the digital signal to the microcontroller via Control PCB.

As shown in Figure 4.5 and appendix, the first amplification stage is a differential amplifier. Since all resistors on the differential amplifier have the same value, the amplifier has a unity gain, where the output of the first stage is equal to the difference of the input. The second, third and fourth stages all are band-pass active filters. The details of the active filters are presented in Figure 4.6. Based on Equation (3.7) and

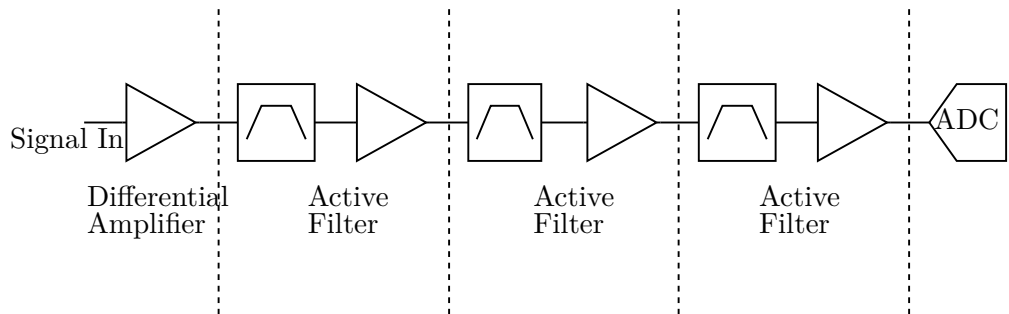


Figure 4.5.: Receiver Filter Stages

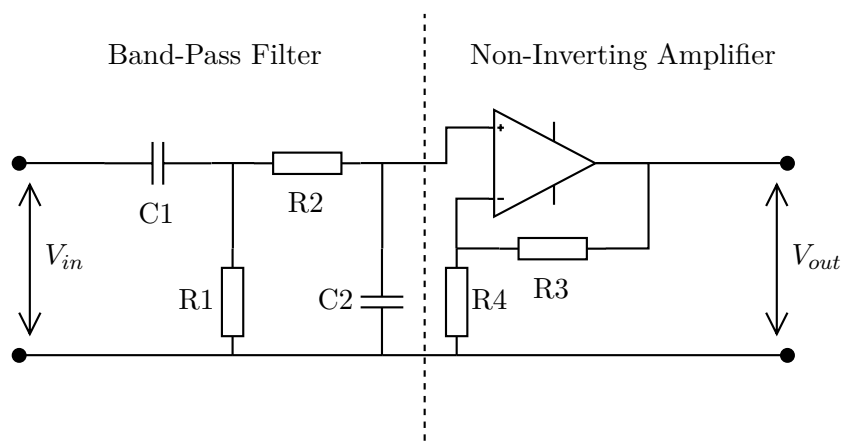


Figure 4.6.: Receiver Active Filter

Equation (3.8) the filter cut off frequencies are:

$$f_L = \frac{1}{2\pi 220 \text{ pF} 100 \text{ k}\Omega} = 7.23 \text{ kHz} \quad (4.3)$$

$$f_H = \frac{1}{2\pi 470 \text{ pF} 12 \text{ k}\Omega} = 28.22 \text{ kHz} \quad (4.4)$$

The center frequency based on Equation (3.9) is:

$$f_r = \sqrt{7.23 \text{ kHz} \cdot 28.22 \text{ kHz}} = 14.28 \text{ kHz} \quad (4.5)$$

The gain for the non inverting amplifier based on Equation (3.12):

$$A_v = 1 + \frac{33 \text{ k}\Omega}{1 \text{ k}\Omega} = 34 \text{ V/V} \quad (4.6)$$

The ADC used in the receiver is ADS8588s, with simultaneous sampling for eight channels, 16-bit resolution using successive approximation analog to digital conversion. The ADC is using synchronous sample and hold mechanism where all channels are sampled simultaneously so that the sample is coherent. The maximum sampling rate is 200 kHz, in this work it is only used for 50 kHz sampling rate. The internal reference used in this configuration is 2.5 V band-gap reference. The pin connection are shown in the Table 4.1.

The pin output DB0-DB15 is connected to PTD0-PTD7 and PTB0-PTB7 to take advantage of the parallel byte communications. By using a connection for each bit, all 16 bits can be transferred at the time. The pin CONVSTA and CONVSTB are shorted and both connected to pin 33 on Teensy 3.6 to start simultaneous sampling of all channels [38].

Table 4.1.: ADS8588s Pin Map

ADS8588s	Teensy 3.6	ARM Cortex-M4
DB0	2	PTD0
DB1	14	PTD1
DB2	7	PTD2
DB3	8	PTD3
DB4	6	PTD4
DB5	20	PTD5
DB6	21	PTD6
DB7	5	PTD7
DB8	16	PTB0
DB9	17	PTB1
DB10	19	PTB2
DB11	18	PTB3
DB12	15	PTB4
DB13	22	PTB5
DB14	23	PTB6
DB15	9	PTB7
RANGE	27	PTA15
STBY	28	PTA16
SEL	29	PTB18
OS2	30	PTB19
OS1	31	PTB10
OS0	32	PTB11
REFSEL	39	PTA17
FRSTDATA	38	PTC11
BUSY	37	PTC10
CS	36	PTC9
SCLK	35	PTC8
RESET	34	PTE25
CONVSTA/B	33	PTE24



Figure 4.7.: Transmitter

Transmitter

The transmitter in the new working configuration is a Teensy 3.6 board with an audio shield for Teensy 3 series. We choose this device for its excellent audio signal processing tools. Although this audio shield normally have enough power and gain to drive small external speaker, an external amplifier is needed because the working frequency used in this work is far from the intended normal operation frequency [39].

External Amplifier

The external amplifier in the working configuration is Visaton amp 2.2 LN which can supply up to 3 W per channel [40]. The volume amplifications can be set manually.



Figure 4.8.: External Amplifier

Power Supply and Hub

The power supply circuit in Figure 4.9 is TPS5430, used to supply balanced dc output of ± 5 V from 12 V battery. The circuit in Figure 4.9 is used to split the power among the microphones and on board amplifier or active filters.

Plate Holder

Figure 4.10 shows the plate holder to fix the distance between microphones and the speaker. The mounting holes in the middle is use for the speaker while the surrounding mount points are for microphones. The distance between mount point diagonally is $10\sqrt{2}$ cm while the vertical and horizontal distances are 20 cm.

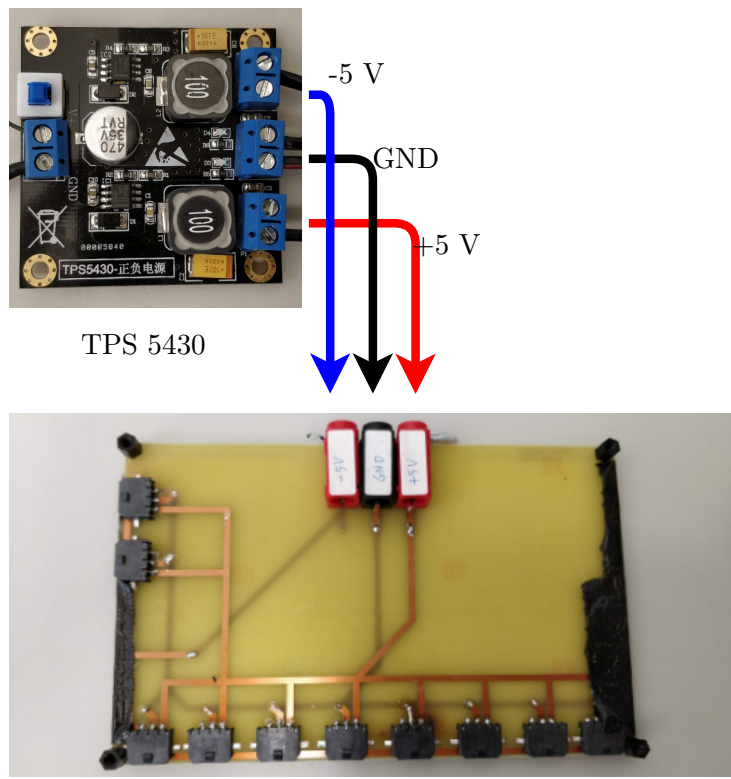


Figure 4.9.: Power Supply

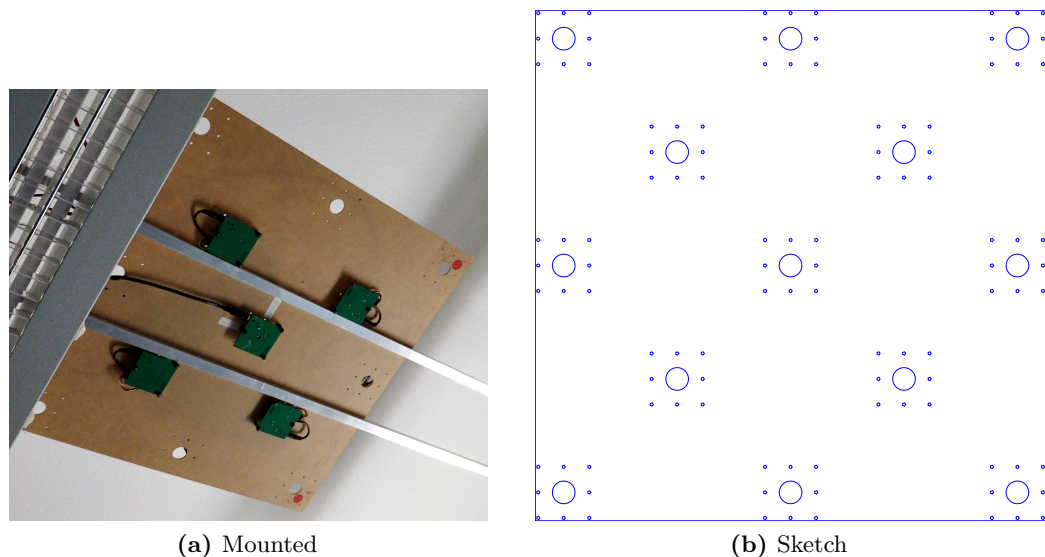


Figure 4.10.: Plate Holder

4.1.2. Software

Transmitter Microcontroller

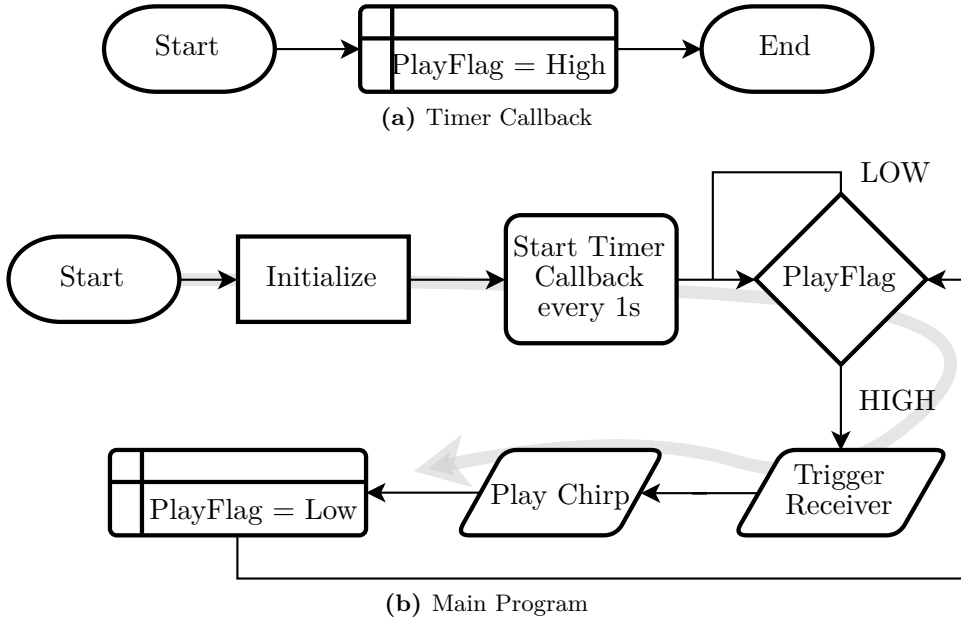


Figure 4.11.: Transmitter Flowchart

The flowcharts in Figure 4.11 show the operation steps of the transmitter. The timer callback function (a) is called every one second. The function simply set the flag to play the chirp up. The main loop (b) continuously check the flag, when the flag is up the transmitter sends the trigger signal to the receiver and play the chirp signal. The chirp signal is generated in PC and converted into sketch of c files which then can be stored inside the microcontroller. The wav files is converted using wav2sketch program from PJRC [39].

Receiver Microcontroller

The flowchart in Figure 4.12 show the algorithm for the receiver microcontroller. The timer callback function (a) is called every 20 ns to achieve 50 kHz sampling rate.

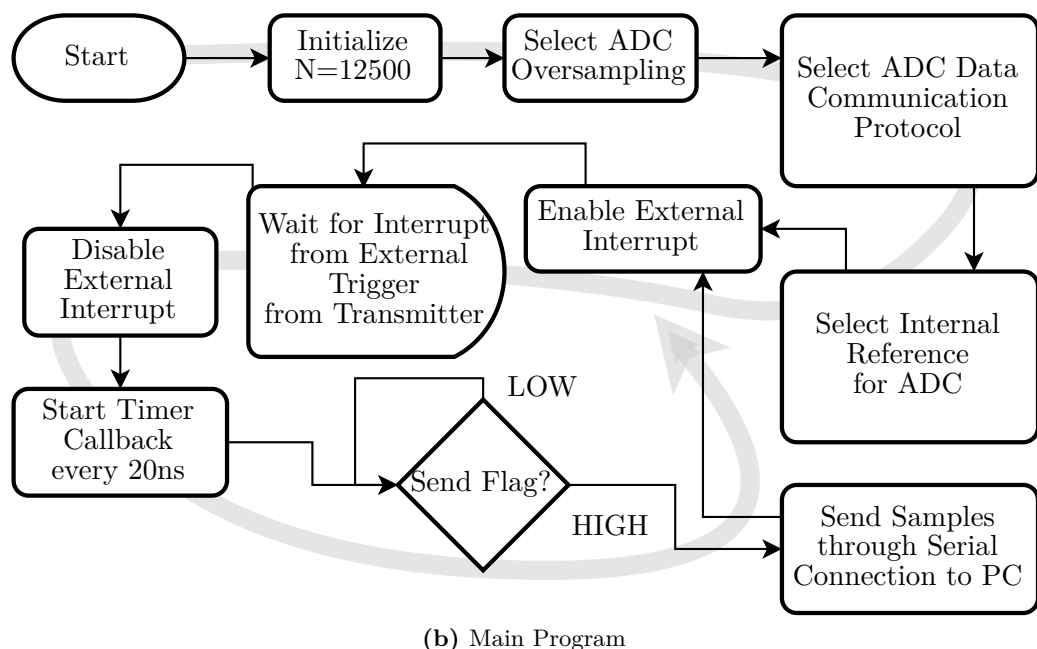
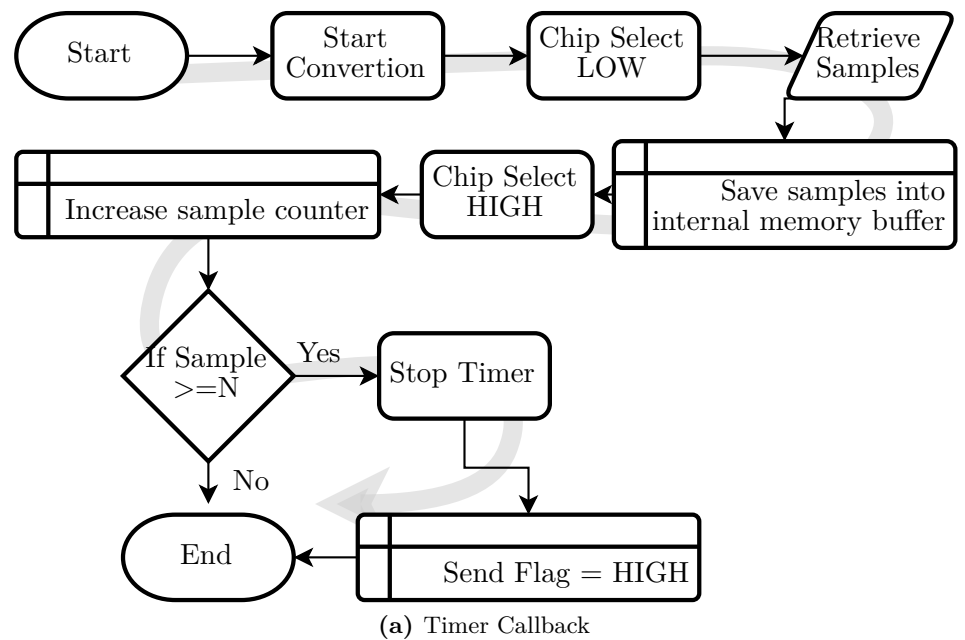


Figure 4.12.: Receiver Flowchart

The clock (SCLK) and chip select (CS) signals are managed in this function. At the end of desired sample number N, the timer is stopped and the send flag is set to high. This flag indicates the samples inside the buffer is ready for transmission to computer via serial connection. The main program (b) is waiting for external interrupt, which indicates a chirp is played, and start recording N samples per channel. Since the duration of recording is 250 ms, the N is set to 12500 as shown below:

$$N = \frac{250 \text{ ms}}{20 \text{ ns}} = 12500 \quad (4.7)$$

Digital Signal Processing

Figure 4.13 present the flowchart of the digital signal processing after the frame received in the computer. First, each frame is verified against missing parts or corrupted signals, then the frame is saved into internal storage. Matched filter is used to determine the phase delay of echoes within the frame by cross correlating the incoming frame against reference signal. Then the room impulse response is derived by calculating the envelope of cross-correlation result. The term impulse response refer to the resulting peaks and the term echo profile refers to the entire envelope signal. The envelope can be derived by calculating the absolute of Hilbert transform of the cross-correlation result. Presence detection and visualization are explained in Section 4.4.

4.1.3. Room Setup

The room used for the experiment is an office room of Laboratory for Electrical Instrumentation(EMP) of IMTEK, Building 71, Room 00 021. At the time of the experiment, the room is conditioned to achieve uniform and repeatable result. The controlled factors are:

- As few clutter as possible - all chairs are removed

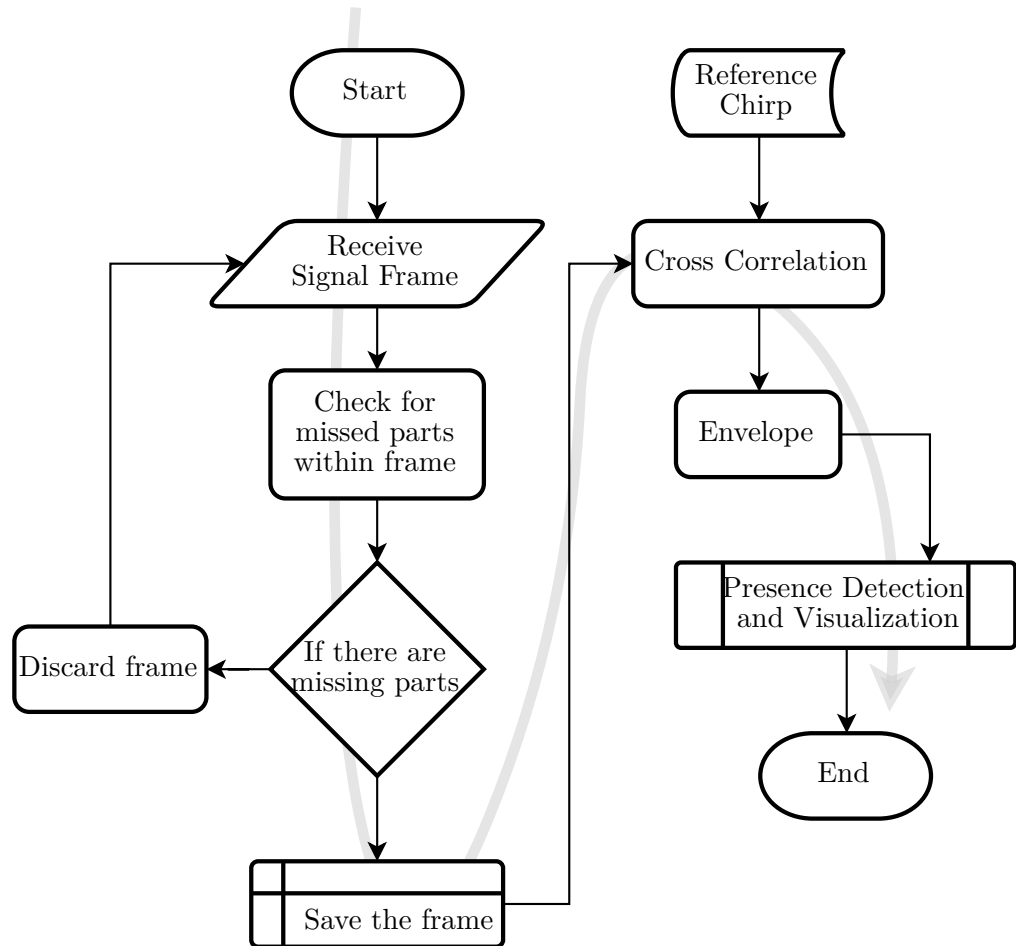


Figure 4.13.: DSP Flowchart

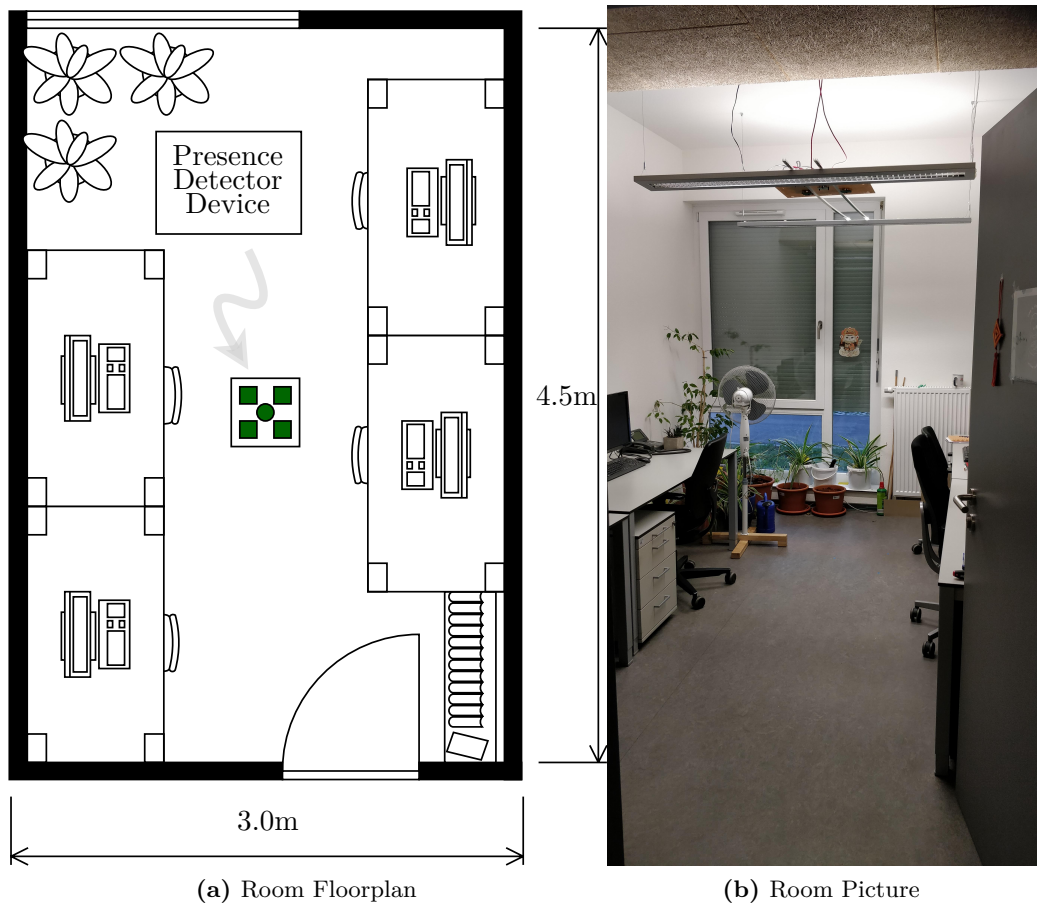


Figure 4.14.: Experiment Room

- Low Noise - quiet environment
- No air current - fans and ventilators are turned off
- Isolated - doors and windows are closed

4.2. Calibration

4.2.1. Speed of Sound

Problem : The speed of sound changes depend on the temperature as shown in Section 3.1. The correct speed of sound is needed to derive correct range of the objects.

Assumption : The air inside the room is isotropic and homogeneous and the temperature stay constant during the experiments.

Approach : Measure the time difference between transmit and received signal for different distances. Use simple constant velocity equation to derive the speed of sound.

4.2.2. Inter-channel Delay

Problem : Each channel has different track length, use different cables and microphones. This caused different delay due to non-uniformity between channels. The received signal have to be synchronized to derive the correct angle of arrival.

Assumption : The delay for each channel is constant and the device has no moving parts.

Approach : Measure the line of sight time of flight for different channel and for different distance. The delay between channel can be calculated with linear regression.

4.3. Chirp Selection

Chirp selection is also an important part, since the channel characteristic were determined empirically, and the resulting multipath echoes are obscuring the desired impulse response, the incoming impulse response is subtracted by empty room echo profile. Since mathematical operation subtraction is used, the variance of impulse response is important to avoid false peaks. Therefore, the chirp are selected by the variance over chirp length.

4.4. Presence Detection

4.4.1. Empty Room Echo Profile

During the experiment, the reflected signals from the floor, walls, tables and chairs has a very high amplitude. This interference can lead to masking the echo from target object. to reduce the effect of the interference, the empty room profile is used to subtract the target impulse response from the input impulse response. If we define the reflection from objects other than target object as noise, we can increase the signal to noise ratio with this method. The empty room impulse response is also called empty room echo profile for this work. In Figure 4.15, the upper plot is the empty room impulse response, where the experiment room is cleared of most clutter. The middle plot is the room with single static object as target, shown in Figure 4.16. The lower plot shows the result of subtraction between the the second and first plot, the scale is adjusted for clarity purpose.

4.4.2. Peak Selection

The peak selection is done with `findpeaks` function in MATLAB. The local maxima location indicate the delay of impulse response from the input frame. As the we seek

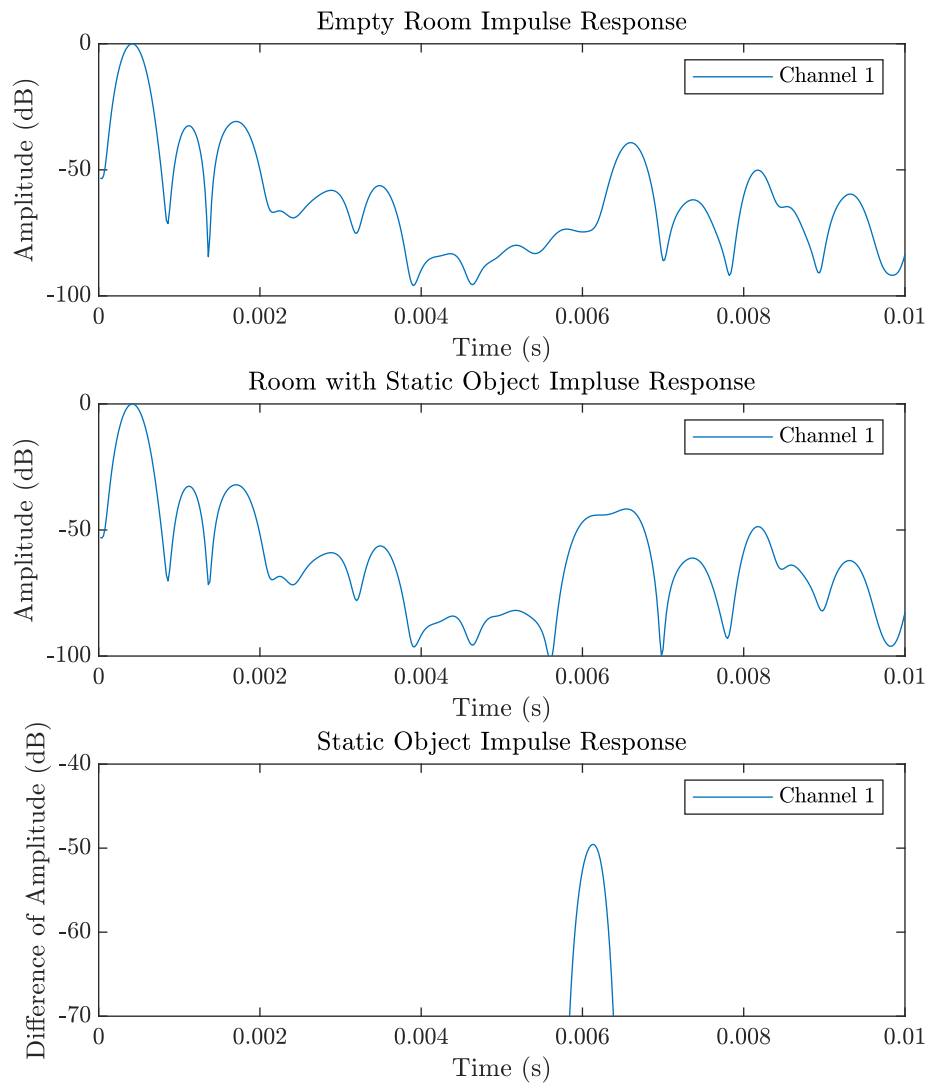


Figure 4.15.: Echo Profiles



Figure 4.16.: Static Object

the peak that caused by the echo wave front, several condition has to be fulfilled:

- The microphones are arranged symmetrically around the speaker, the average of time of arrival of a single chirp to microphone of the opposite side must be the same. From the arrangement in Figure 4.19, the following condition must be fulfilled:

$$\frac{t_1 + t_3}{2} = \frac{t_2 + t_4}{2} \quad (4.8)$$

- The maximum difference between time of arrivals from microphones of opposite side must not exceed:

$$t_{maxO} = \frac{0.2\sqrt{2} \text{ m}}{c} \quad (4.9)$$

Where c is the speed of sound.

- The maximum difference between time of arrivals from microphone side by side must not exceed:

$$t_{maxS} = \frac{0.2 \text{ m}}{c} \quad (4.10)$$

Where c is the speed of sound.

- The time of arrivals from all microphone have to exceed the line of sight travel time.

4.4.3. Distance Map

The distance map is a matrix generated beforehand to minimize the processing time within the program. The matrix act as pointer to convert binary sampling point into distance point. The matrix contain the sum of distance between each point to microphones and to the speaker, which cover the flight path of the echoes.

$$M_{Total} = M_T + M_R \quad (4.11)$$

Where M_T is the distances between microphones to the object and M_R is the distance between the center of the device with the object. The matrix size correspond to the area of detection.

4.4.4. Direct Intersections

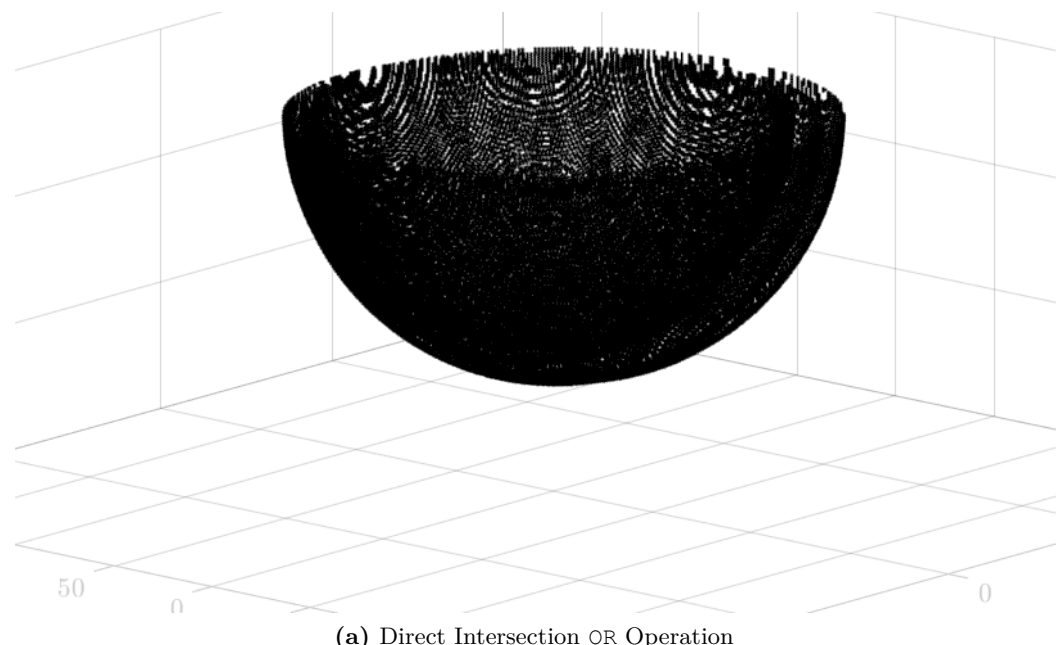
Direct intersection is a very simple visualization method where the distance map matrix is used to map out the peaks for each microphone, and then use simple AND operation to intersect the possible source point. Then the resultant matrix can be displayed as a pointcloud. Figure 4.17 displays the result of this method. In the upper figure (a) the OR operation is used to show the four half semi-spherical pattern are the result of the wave impulse response mapped into 3D space. In the lower figure (b) the result of AND operation is shown. This is the detected reflection from object depicted in Figure 4.16.

4.4.5. Sonogram

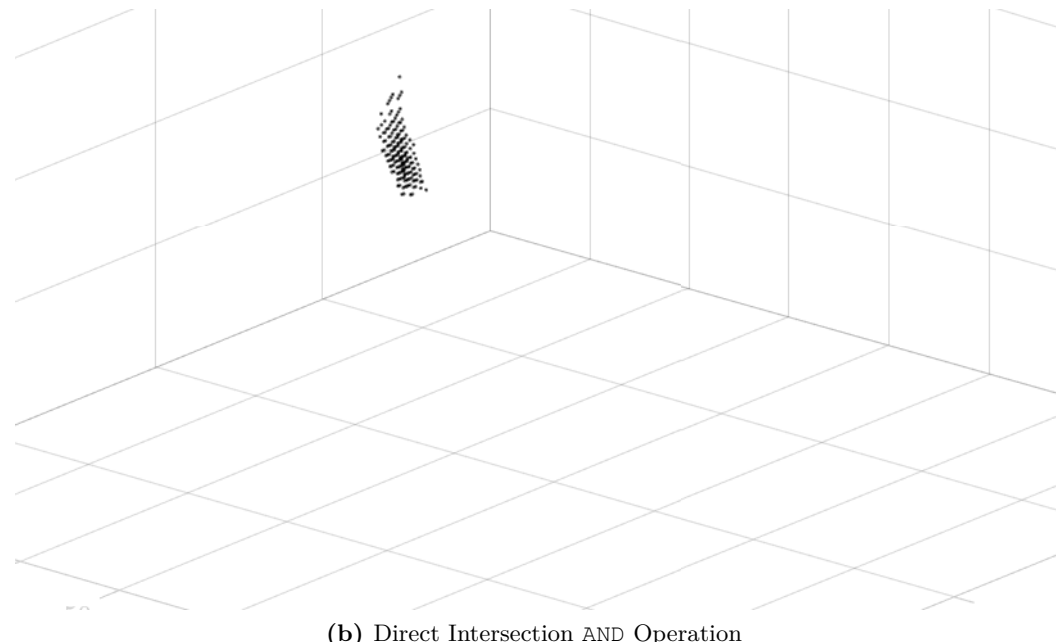
The sonogram display is created by mapping the entire impulse response into the distance map, resulting in 3D intensity map. However such map would take considerable amount of memory and processing power. Moreover it is quite hard to visualize and display such data in convenient way. Therefore the sonogram is only used to create a 2D intensity map, which can then be displayed. Figure 4.18 depict the sonogram of reflection from object shown in Figure 4.16.

4.4.6. Angle of Arrival and Time of Flight Estimation

To estimate the angle of arrival with the assumption that the incoming waves is a planar waves, the azimuths and elevations can be calculated based on the time difference of arrivals as illustrated in Figure 4.20. The range can be calculated as



(a) Direct Intersection OR Operation



(b) Direct Intersection AND Operation

Figure 4.17.: Direct Intersection

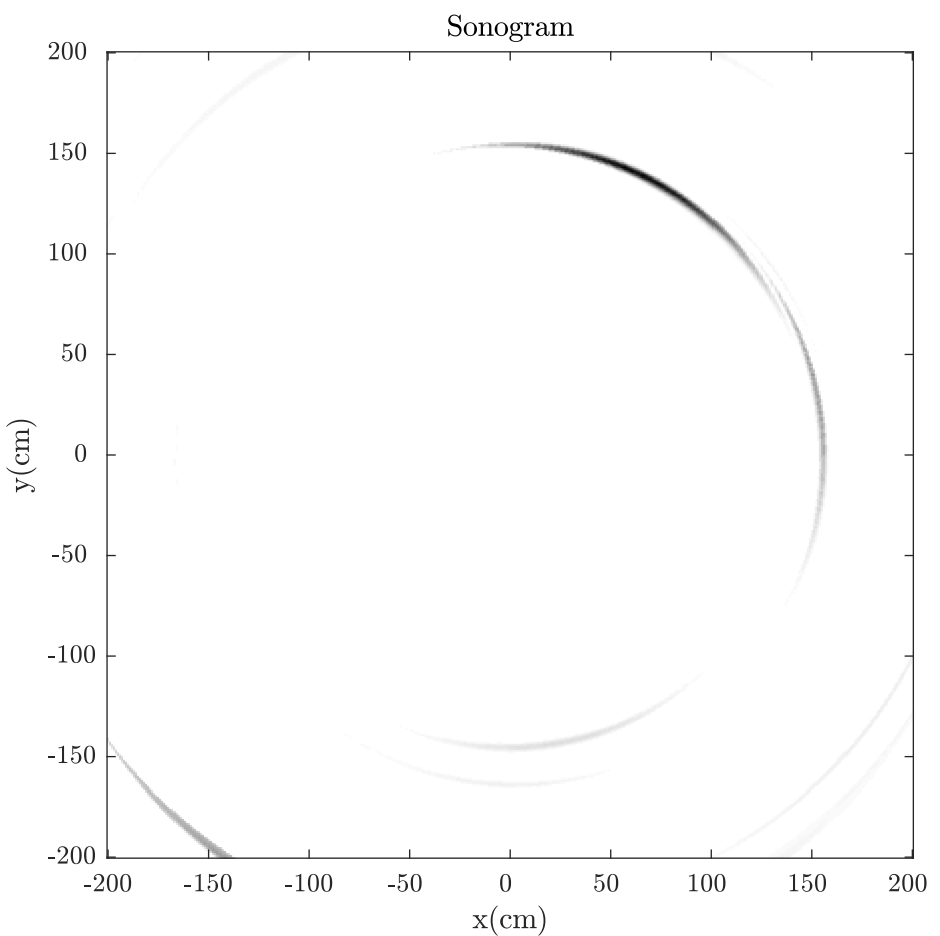


Figure 4.18.: Sonogram

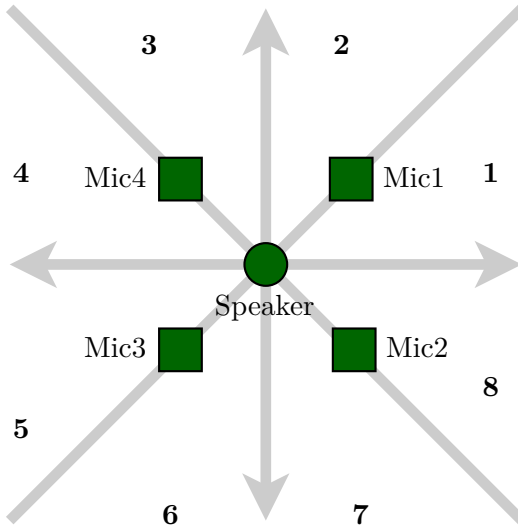


Figure 4.19.: Octant Division

half of the mean of time of flights, since the microphones arrangement is symmetric around the speaker and the time of flights from speaker to object is the same as from the object back to the device.

$$r = \frac{t_1 + t_2 + t_3 + t_4}{4 \cdot 2} \quad (4.12)$$

The location of the speaker on the center of the device is used as reference point for all distance calculation. The azimuth ϕ in Figure 4.21 can be calculated per octant as:

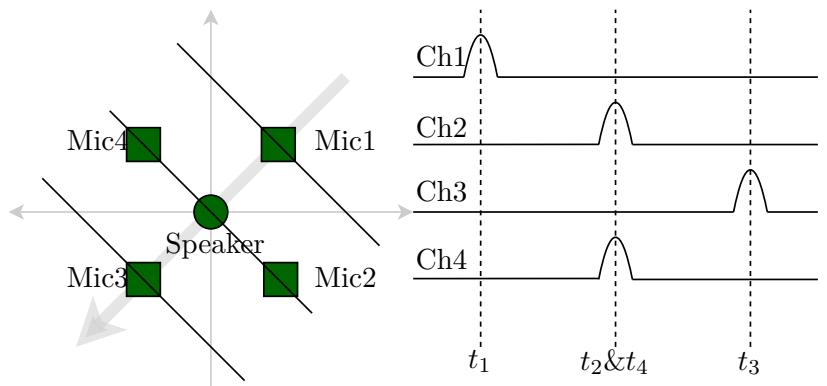
$$\cos\left(\frac{\pi}{4} - \phi\right) = \frac{dt_1}{r} \quad (4.13)$$

$$\cos\left(\frac{\pi}{4} + \phi\right) = \frac{dt_2}{r} \quad (4.14)$$

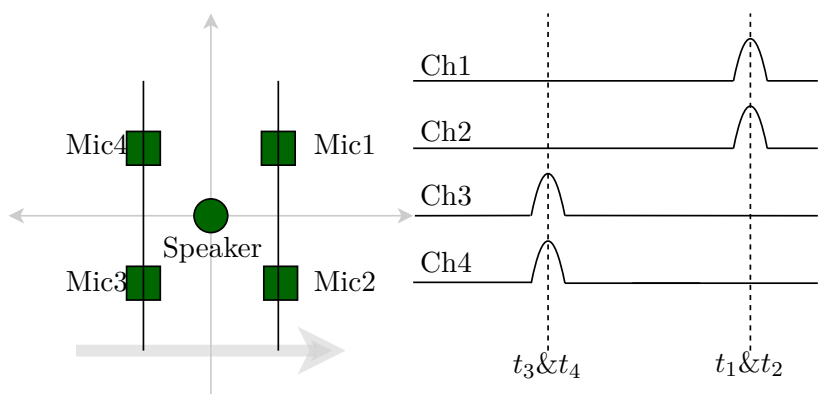
dt_1 and dt_2 are half the difference between time of arrival from opposite microphones.

$$\frac{dt_1}{dt_2} = \frac{\cos\left(\frac{\pi}{4} - \phi\right)}{\cos\left(\frac{\pi}{4} + \phi\right)} \quad (4.15)$$

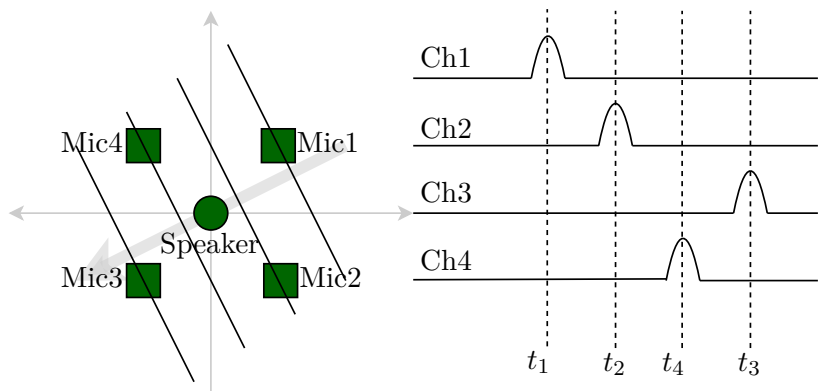
$$\frac{dt_1}{dt_2} = \frac{\cos\left(\frac{\pi}{4}\right)\cos(\phi) + \sin\left(\frac{\pi}{4}\right)\sin(\phi)}{\cos\left(\frac{\pi}{4}\right)\cos(\phi) - \sin\left(\frac{\pi}{4}\right)\sin(\phi)} \quad (4.16)$$



Diagonal Wavefront Impulse Response Timing
(a) Diagonal Azimuth



Parallel Wavefront Impulse Response Timing
(b) Parallel / Cardinal Azimuth



First Octant Wavefront Impulse Response Timing
(c) First Octant Azimuth

Figure 4.20.: Wave front Azimuth

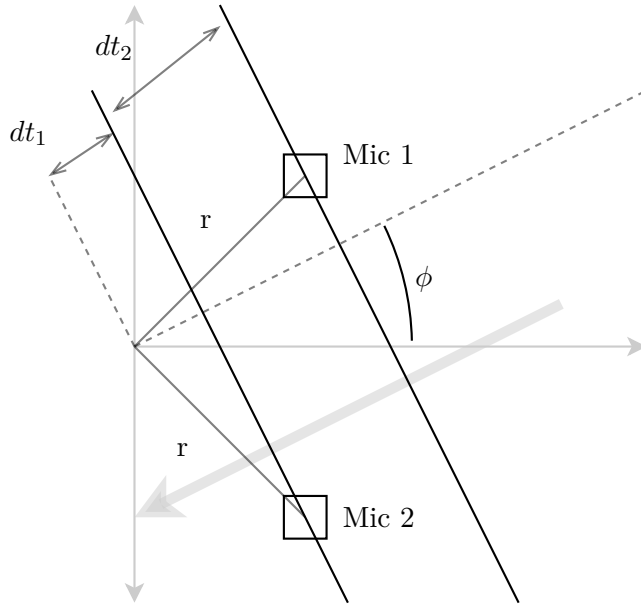


Figure 4.21.: Azimuth

$$\frac{dt_1}{dt_2} = \frac{\cos(\phi) + \sin(\phi)}{\cos(\phi) - \sin(\phi)} \quad (4.17)$$

$$\frac{dt_1}{dt_2} = \frac{\cos(\phi) + \sin(\phi)}{\cos(\phi) - \sin(\phi)} \cdot \frac{\frac{1}{\cos(\phi)}}{\frac{1}{\cos(\phi)}} \quad (4.18)$$

$$\frac{dt_1}{dt_2} = \frac{1 + \tan(\phi)}{1 - \tan(\phi)} = \frac{\tan(\frac{\pi}{4}) + \tan(\phi)}{1 - \tan(\phi)\tan(\frac{\pi}{4})} = \tan(\frac{\pi}{4}) + \phi \quad (4.19)$$

$$\text{atan}(\frac{dt_1}{dt_2}) = \phi + \frac{\pi}{4} \quad (4.20)$$

$$\phi = \text{atan}(\frac{dt_1}{dt_2}) - \frac{\pi}{4} \quad (4.21)$$

The elevation θ also can be calculated from Equation (3.4) that:

$$\theta = \text{acos}(\frac{c \cdot (dt_1 - dt_2)}{(cos(\frac{\pi}{4} - \phi) \cdot r) - (cos(\frac{\pi}{4} - \phi) \cdot r)}) \quad (4.22)$$

Keep in mind that the elevation is negative and only between zero to $\frac{\pi}{2}$ rad due to the positioning of the device. There are also special cases where the direction of incoming waves is exactly diagonal or parallel, or in one specific case where the

direction of the waves is perpendicular to the device. In these cases a separation based on the timing can be used to determine the spherical coordinates.

4.5. Retired Configuration

From Figure 4.2 (a), the retired configuration has different controller and different transmitter. Retired hardware shown in Figure 4.22 and Figure 4.23 has been depreciated since the preliminary experiment. In this section these parts are discussed for completion purpose.

4.5.1. Control

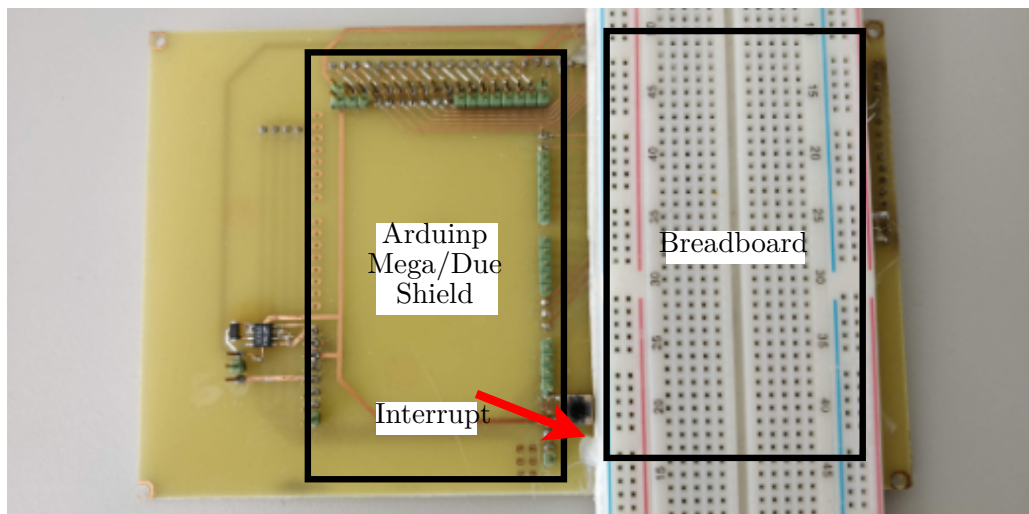


Figure 4.22.: Retired Control

This control board shown in Figure 4.22 is used for testing Arduino Mega 2560 and Arduino Due as a shield, as well as Arduino MKR Zero on the breadboard. The external interrupt is connected to a push button for testing purposes. Pin connections list are shown in Table 4.2.

Table 4.2.: Retired Control Pin Connection

ADS8588s	Arduino Mega 2560
DB0	23
DB1	25
DB2	27
DB3	29
DB4	31
DB5	33
DB6	35
DB7	37
DB8	39
DB9	41
DB10	43
DB11	45
DB12	47
DB13	49
DB14	51
DB15	53
RANGE	24
STBY	26
SEL	28
OS2	30
OS1	32
OS0	34
REFSEL	52
FRSTDATA	50
BUSY	48
CS	46
SCLK	44
RESET	42
CONVSTA	22
CONVSTB	40

4.5.2. Transmitter

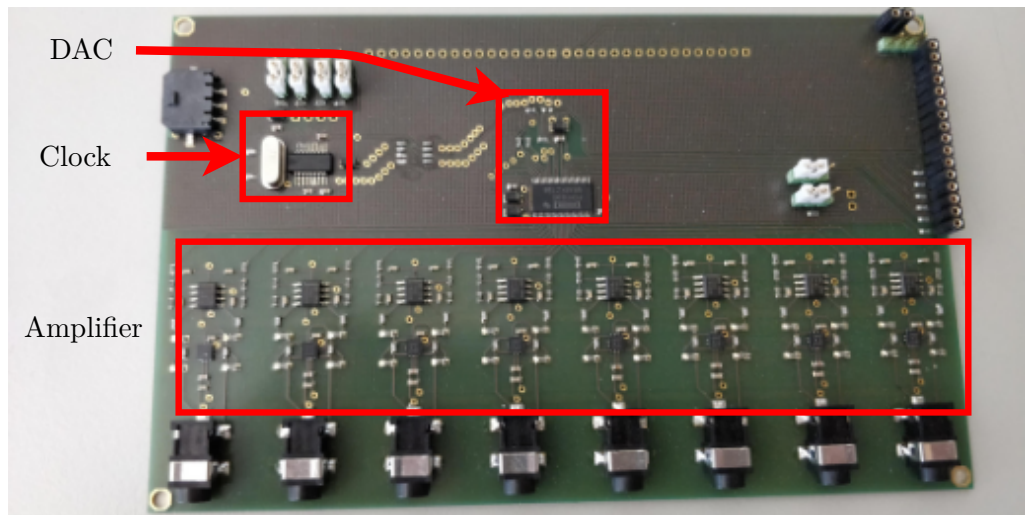


Figure 4.23.: Retired Transmitter

The transmitter board in Figure 4.23 is an eight channel audio output device. The DAC used in this board is PCM1690. The DAC is able to receive digital sound signal via SPI from micro controller, the clock is used to drive both the communication and the sampling rate of the DAC. Several main reason why this part is shelved:

- One of the steering parameters of beamforming is the frequency. As the chirp has a wideband frequency an adaptive wideband beamforming algorithm may be needed instead of simple phase shift delay.
- Surround sound techniques also can be used, however by focusing constructive interference at target location does not necessarily means the reflected signal is composed as a single impulse or chirp. Ideally, the constructive interference should happen after reflection, at the receiver. However to do this, the location of reflective surface have to known, which defeat the localization purpose of the device.

Due to these uncertainties and low returns these parts are shelved for now. In the

future, it might be a good idea to develop an acoustic beamforming transmitter.

5. Experiments

In this chapter the experiment setups are described and the results are displayed. Before the device is ready for the localization and tracking experiment, device characterization and calibration has to be done. Section 5.1 describe the characterization of the device and Section 5.2 describe the calibration of the device. Section 5.3 detailed the chirp selection process. The experiments for presence detection are described in Section 5.4, this experiments shows the accuracy of the device, dependency of target surface and the visualization result.

5.1. Hardware Validation

5.1.1. Speaker and Microphones

Figure 5.1 shows the setup and arrangement of the experiments. The purpose of this experiments is to validate the speaker and microphones frequency responses using the sine sweep method. A sinusoidal frequency modulated signal is generated from the computer, and played through the speaker. The signal is a 5 kHz to 25 kHz chirp with raised cosine window, the chirp duration is 20 s as mentioned in Section 4.3. Each experiment done with 10 consecutive chirps with 20 s silent period in between. As shown in Figure 5.1, the experiments is done inside an anechoic chamber. Distance d between speaker and microphone is set to 30 cm. Audio interface Focusrite

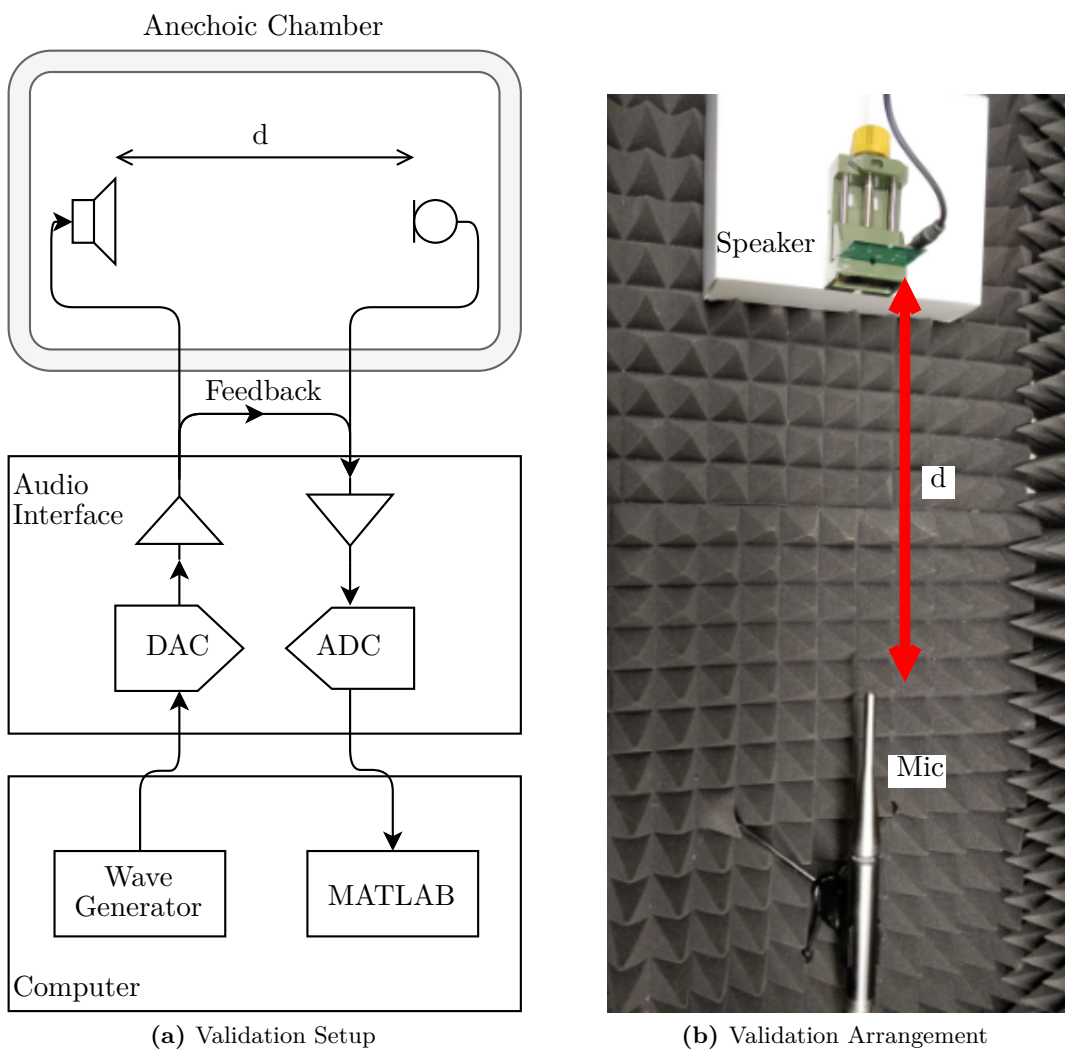


Figure 5.1.: Hardware Validation

Scarlett 18i20 2nd Gen is used for transmitting and recording the acoustic wave. The sampling frequency is 96 kHz.

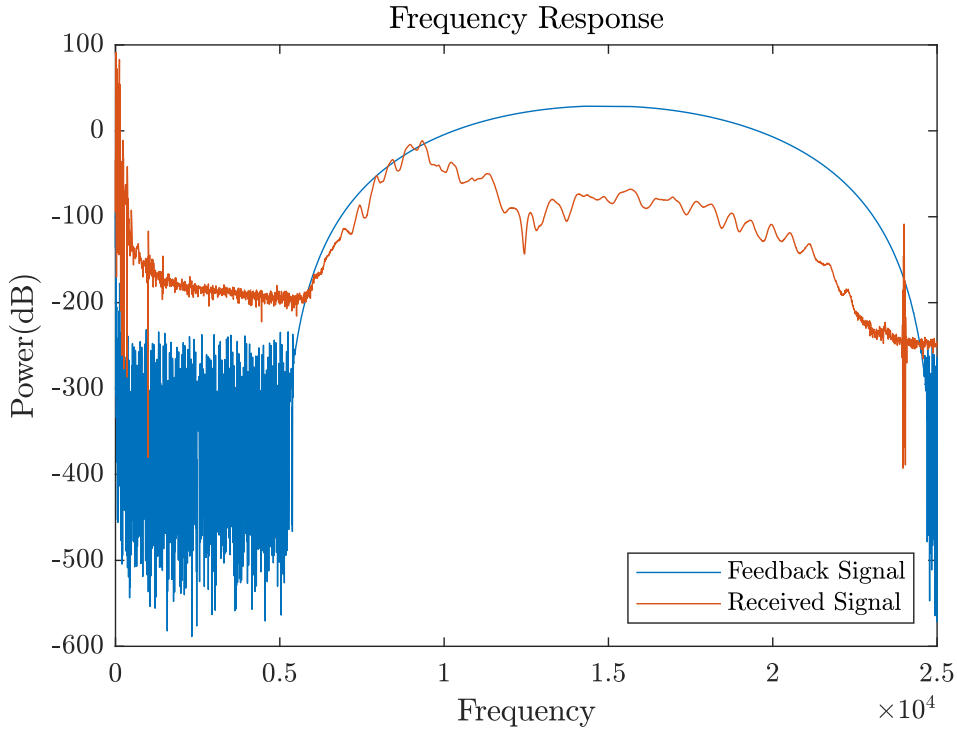


Figure 5.2.: Frequency Response of Speaker vs Reference Microphone

As can be seen on figure Figure 5.2, the frequency response of the speaker against reference microphone start to decline at around 10 kHz frequency. The microphone that is used in the experiment has build in pre-amplifier as mentioned in Section 4.1.1. The frequency responses of the speaker against the microphones is shown in Figure 5.3. The responses shows significant improvement around 18 kHz frequency as well as moderate amplification from 15 kHz to 24 kHz.

5.1.2. Pre-Amplifiers

The pre-amplifier is regarded as device under test in the setup described in Figure 5.4. Figure 5.5 shows the result of pre-amplifier test. the sine sweep signal used is a linear

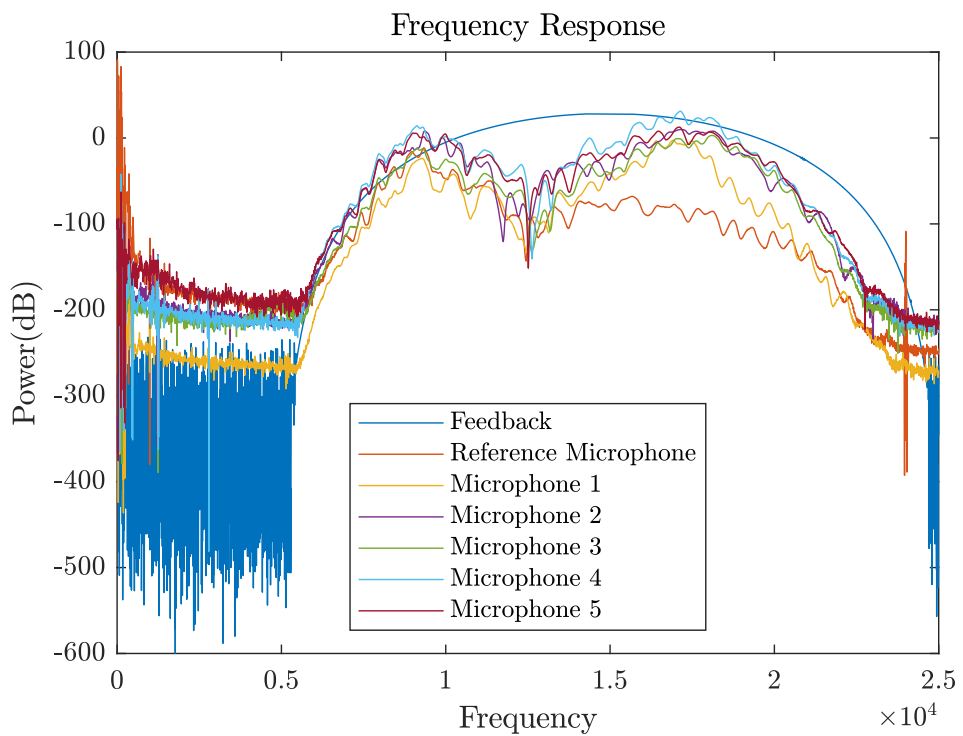


Figure 5.3.: Frequency Responses

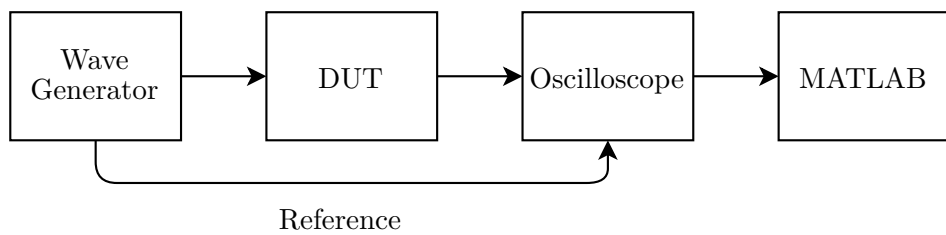
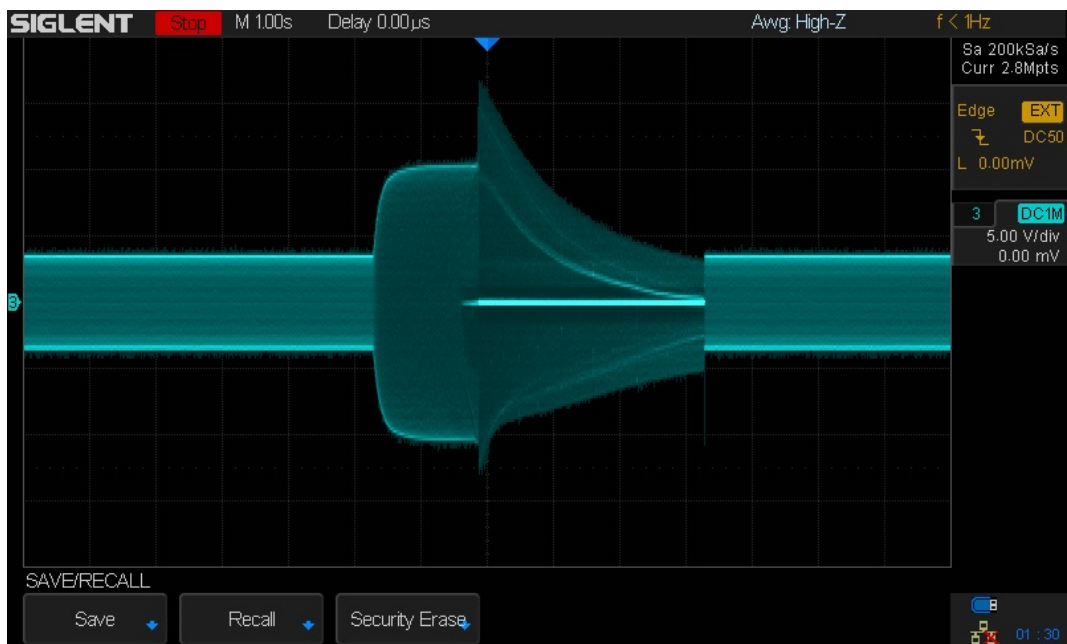
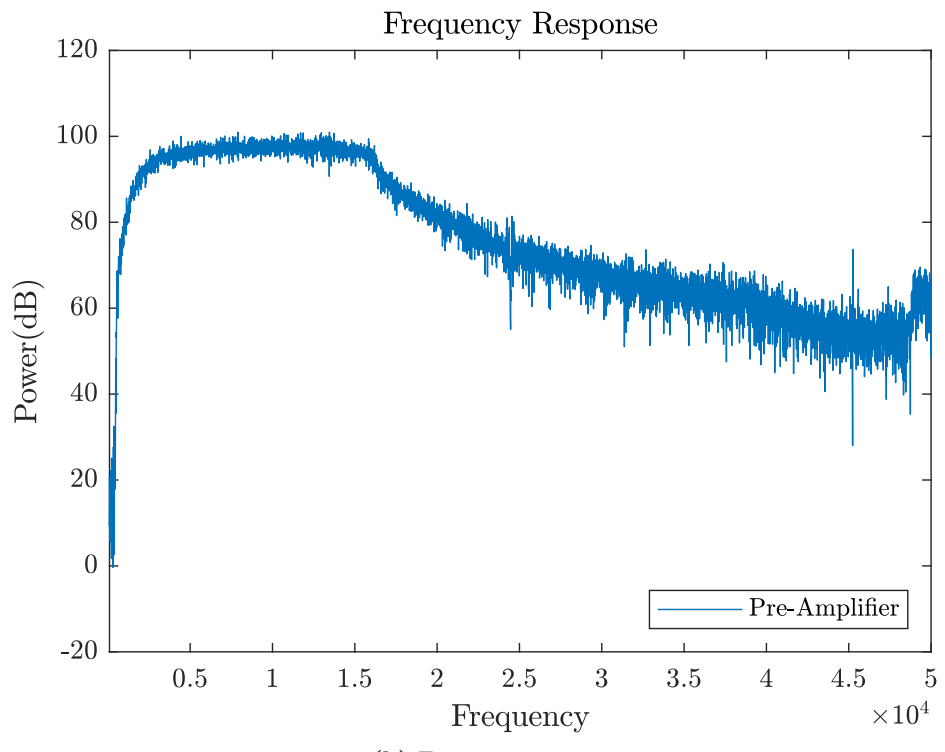


Figure 5.4.: Setup for Sine Sweep Test The sine sweep test using wave generator and oscilloscope for pre-amp and filters.



(a) Sine-sweep response



(b) Frequency response

Figure 5.5.: Pre-Amplifier

up-chirp from 500Hz to 50kHz, with 5 s duration. The oscilloscope probe is set for 10 times magnification. The steady state is approximately at 5 V. At higher frequency the pre-amplifier shows attenuation due to op-amp characteristics. The Figure 5.5 also shows the frequency response of the pre-amplifier.

5.1.3. Active Filters

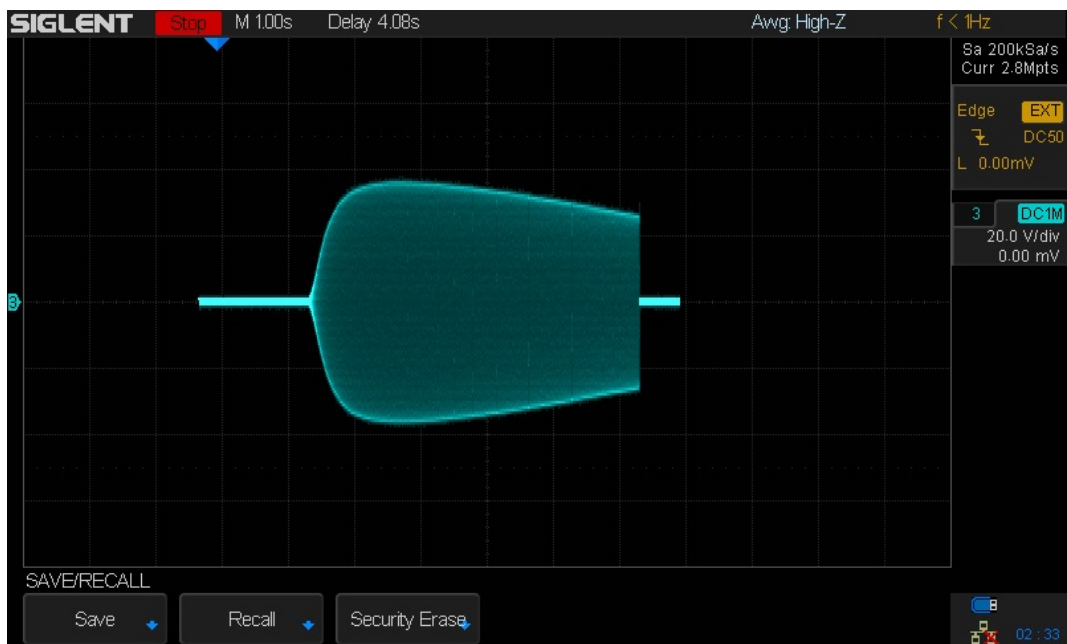
With similar setup described in Figure 5.4, now the active filters of the receiver is regarded as the device under test. Due to higher amplification, the sine sweep amplitude is reduced to 25 mV. Even so, due to the amplifier, the voltage reach 4 V. Keep in mind that the probe has ten times magnification. The oscilloscope display and the frequency response can be seen in Figure 5.6.

5.1.4. ADC

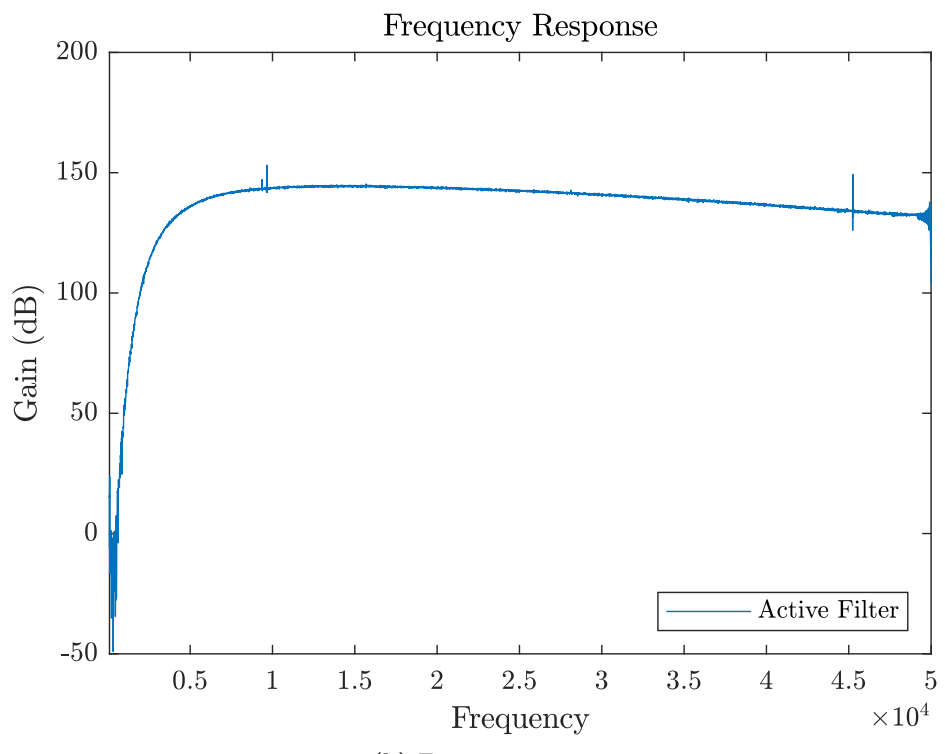
This subsection is intended for the validation of the ADC, however due to the unique built of the device, the ADC cannot record continuously, instead the device capture a set of "frame" or a certain period of recording, synchronized with the transmitter. Therefore to validate the device, the direct feedback channel from transmitter to the receiver is used to transmit a relatively long chirp. The chirp duration is 200 ms long and the frequency goes up from 2 kHz to 22 kHz. Raised cosine window is used to smooth out the transmission of the chirp.

5.1.5. Concluding Remarks

The device is able to perform the intended purpose, the active filter can balanced out the attenuation due to out of specification working frequency. Although the speaker works well up to 10 kHz, external amplifier has to be used to improve signal strength for higher frequency. The microphones actually has better frequency



(a) Sine-sweep response



(b) Frequency response

Figure 5.6.: Pre-Amplifier

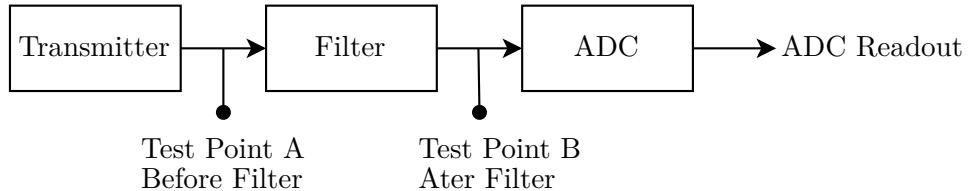


Figure 5.7.: ADC Validation Setup

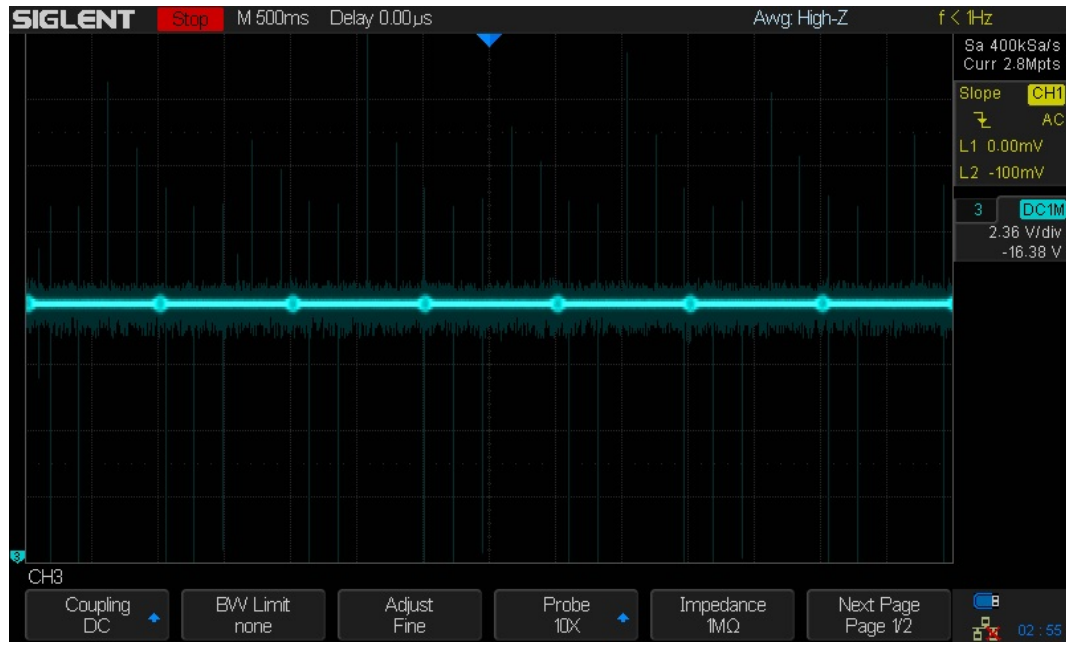
response compared to the reference microphone at higher frequency, due to included pre-amplification stage.

5.2. Device Calibration

The purpose of device calibration is to improve accuracy of the system by calculating the current speed of sound and the delay between input channels. Figure 5.11 shows the setup and arrangement of the calibration process. Chirp sound is played 100 times for each microphones and distances setup, the distances and time of flights are shown in Table 5.1. The time of flights are calculated based on the difference between matched filter of feedback signal and received signal. A simple linear regression is used to determine speed of sound and the delay between channels.

Table 5.1.: Calibration Result Time of Flight (ToF) of direct line of sight from calibration setup.

Distance (cm)	20	25	30	35	40	45	50	55	60	65
ToF Ch.1 (ms)	0.66	0.79	0.93	1.08	1.23	1.37	1.55	1.68	1.81	1.95
ToF Ch.2 (ms)	0.68	0.86	0.98	1.13	1.30	1.42	1.60	1.74	1.87	2.01
ToF Ch.3 (ms)	0.72	0.86	1.01	1.16	1.30	1.44	1.60	1.76	1.88	2.03
ToF Ch.4 (ms)	0.69	0.84	0.97	1.12	1.26	1.42	1.58	1.72	1.86	2.00



(a) Before Active Filter



(b) After Active Filter

Figure 5.8.: Channel test

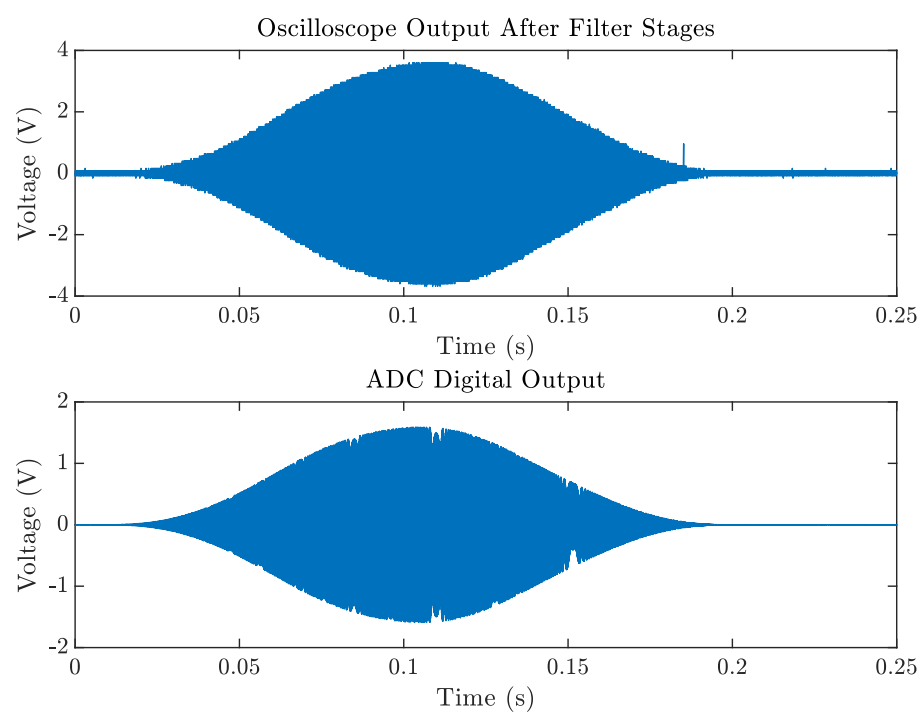


Figure 5.9.: Measured Signal and Digital Readout

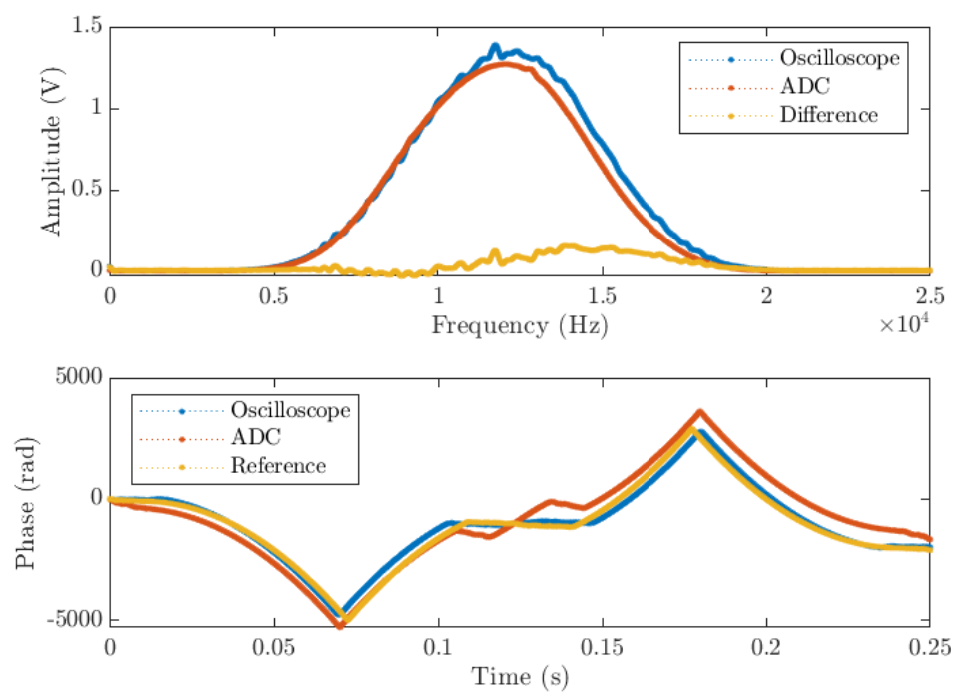


Figure 5.10.: ADC Amplitude Spectrum

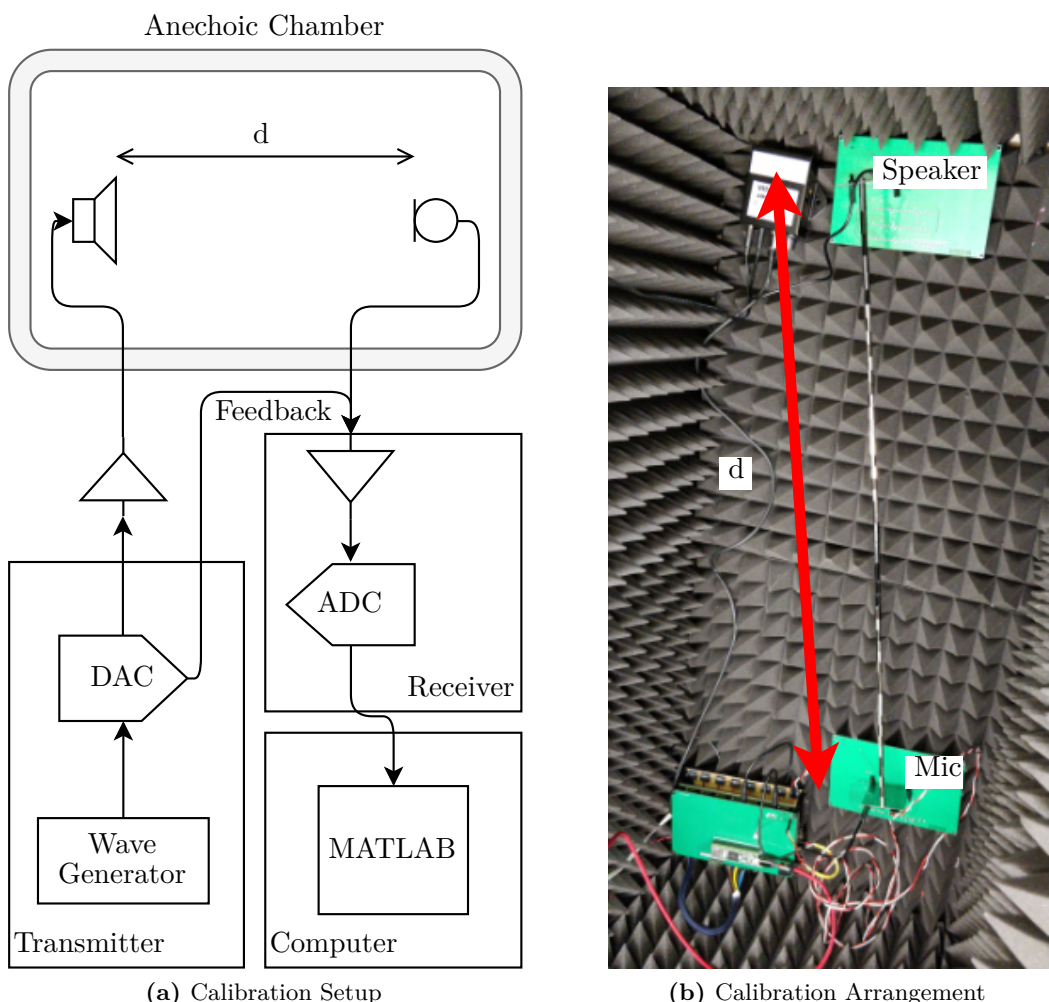


Figure 5.11.: Device Calibration

5.2.1. Inter-channel Delay

The inter-channel delays are calculated by simple linear regression method. Keep in mind that with the assumption of constant and isotropic speed of sound, the equation for is linear:

$$\Delta d = c \cdot \Delta t \quad (5.1)$$

Where d is distance, c is the speed of sound and t is elapsed time. Table 5.1 contain the time of flight and the distance travelled by acoustic wave. Therefore by extrapolating with linear regression the difference in time due to channel delay can be derived by calculating the Δt zero distance. The linear regressions are:

$$d_1 = 342.78 \text{ m s}^{-1} \cdot t_1 - 22.33 \text{ m}$$

$$d_2 = 338.19 \text{ m s}^{-1} \cdot t_2 - 34.60 \text{ m}$$

$$d_3 = 341.65 \text{ m s}^{-1} \cdot t_3 - 45.11 \text{ m}$$

$$d_4 = 340.51 \text{ m s}^{-1} \cdot t_4 - 33.32 \text{ m}$$

Therefore the time differences at zero distance are:

$$t_1 = \frac{22.33 \text{ m}}{342.78 \text{ m s}^{-1}} = 0.065 \text{ s}$$

$$t_2 = \frac{34.60 \text{ m}}{338.19 \text{ m s}^{-1}} = 0.102 \text{ s}$$

$$t_3 = \frac{45.11 \text{ m}}{341.65 \text{ m s}^{-1}} = 0.123 \text{ s}$$

$$t_4 = \frac{33.32 \text{ m}}{340.51 \text{ m s}^{-1}} = 0.098 \text{ s}$$

5.2.2. Speed of Sound

As can be seen in the linear regression results, the slope of the linear equations are the speed of sound. The average of all the slope is:

$$c_{meas} = \frac{342.78 + 338.19 + 341.65 + 345.11}{4} \cdot 10^0 \text{ m s}^{-1} = 340.78 \text{ m s}^{-1} \quad (5.2)$$

At the time of the experiment, the temperature inside the box is 290.55 K. Then theoretically the speed of sound should be:

$$c_{air} = 20.05 \text{ m s}^{-1} \text{ K}^{-\frac{1}{2}} \cdot \sqrt{290.55 \text{ K}} = 341.76 \text{ m s}^{-1} \quad (5.3)$$

5.2.3. Concluding Remarks

In the application, the delay between channel can be calculated as a sampling difference instead of time, since the sampling rate is constant and the sampling of all channel is synchronous. The inter-channel delay is constant as long as the configuration is fixed. The measured speed of sound is quite close compared to the theoretical value. The difference of less than one m s^{-1} or about one percent.

5.3. Chirps

Figure 5.12 shows the setup and arrangement for chirp selection. The reference microphone is used in this experiment, the distance between the speaker and the reference microphone is fixed at 30 cm. Several different chirps are transmitted 150 times each in consecutive cycles to avoid long term drift. The purpose of the chirp selection is to find chirp parameter with lowest standard deviation after cross-correlation envelope process and to avoid artifact peaks due to unstable transmission. Eight different chirps are evaluated in this section, four with 10 kHz bandwidth and

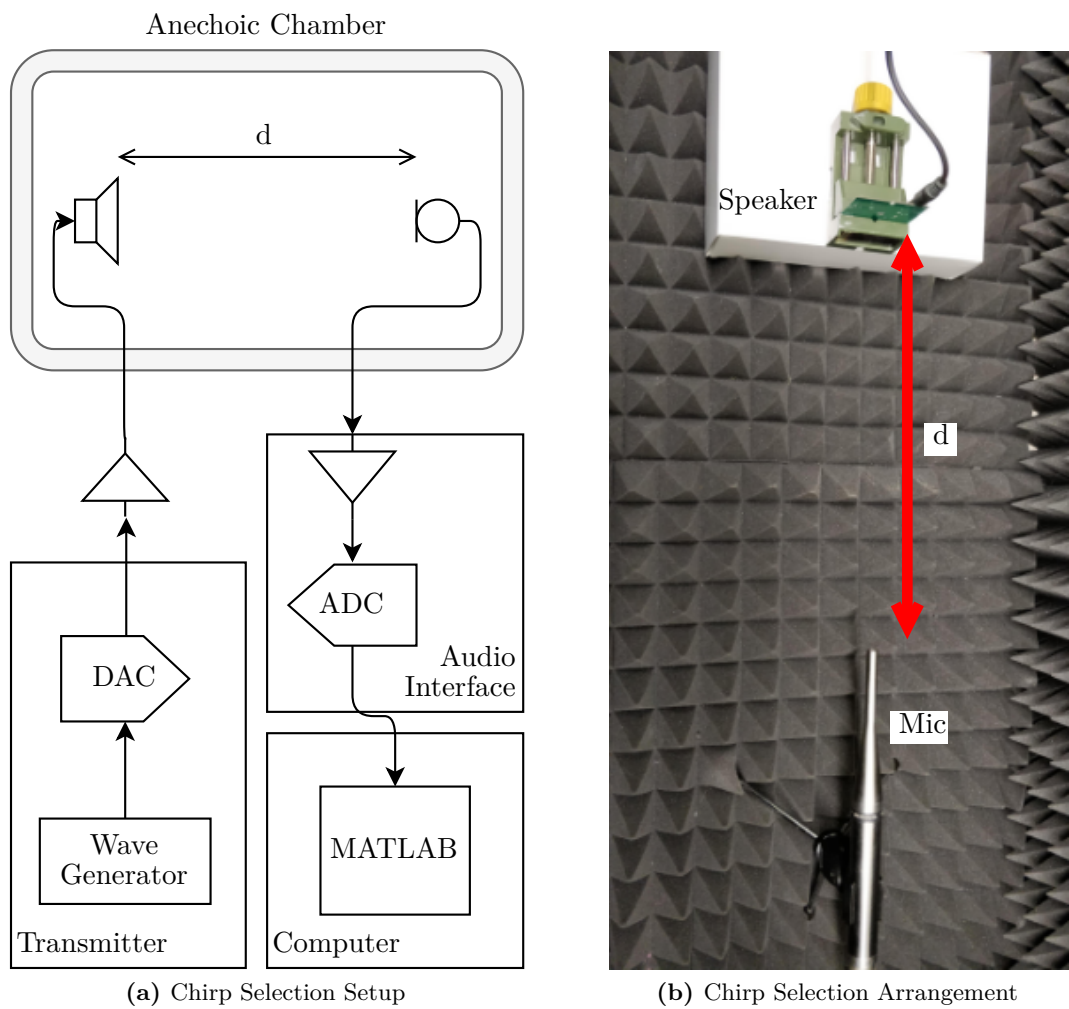


Figure 5.12.: Chirp Selection Experiment

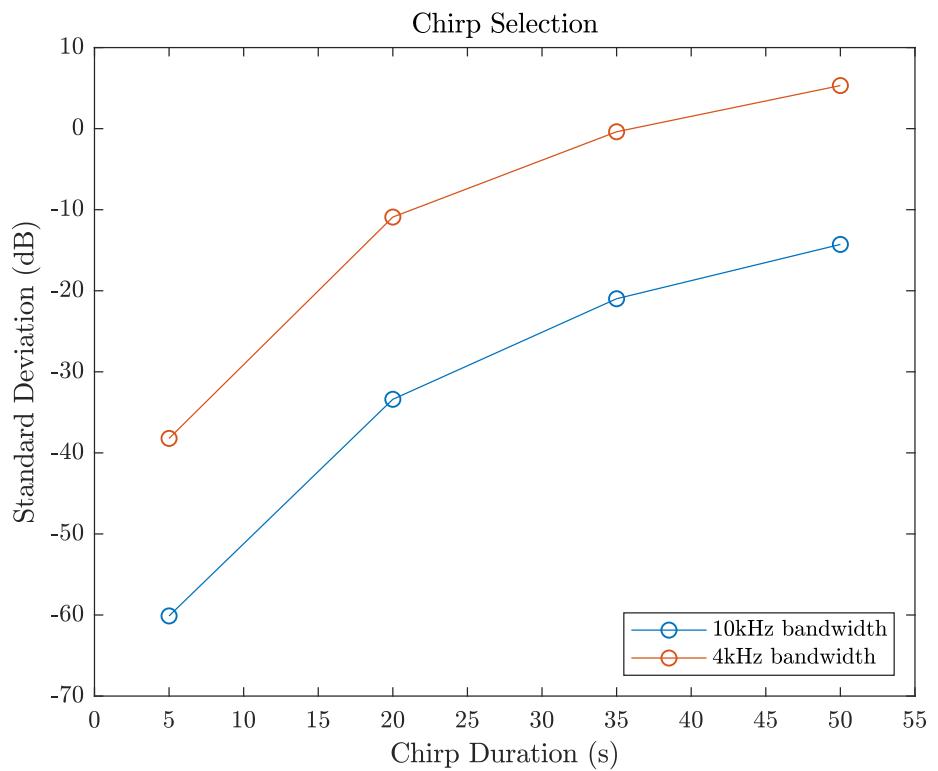


Figure 5.13.: Chirp Selection Result

four with 4 kHz bandwidth. They are further divided into 5 ms, 20 ms, 35 ms, and 50 ms lengths respectively.

5.3.1. Concluding Remarks

As can be seen in Figure 5.13, the chirp with lower duration and higher bandwidth have lower standard deviation. However due to the hardware limitation, a chirp with 10 kHz bandwidth has to be in audible frequency. To avoid audible frequency range, the chirp used in consequent experiment is an up-chirp from 16 kHz to 22 kHz with 6 kHz bandwidth and duration of 5 ms.

5.4. Presence Detection

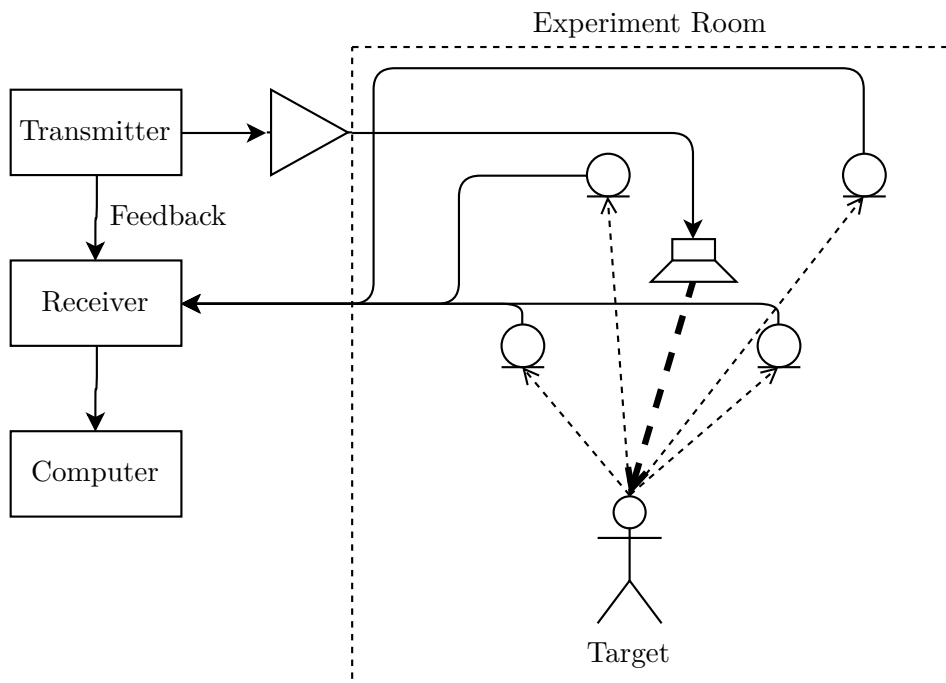


Figure 5.14.: Experiment Setup

Figure 5.14 shows the setup of the experiment. The device is ceiling mounted as shown in Figure 4.16. The location of the device and the room outline is shown in Figure 4.14. Figure 4.13 shows the simplified signal processing up to this point. In this section the presence detection and visualization methods mentioned in Section 4.4 are used to derive the location of target object.

5.4.1. Static Object

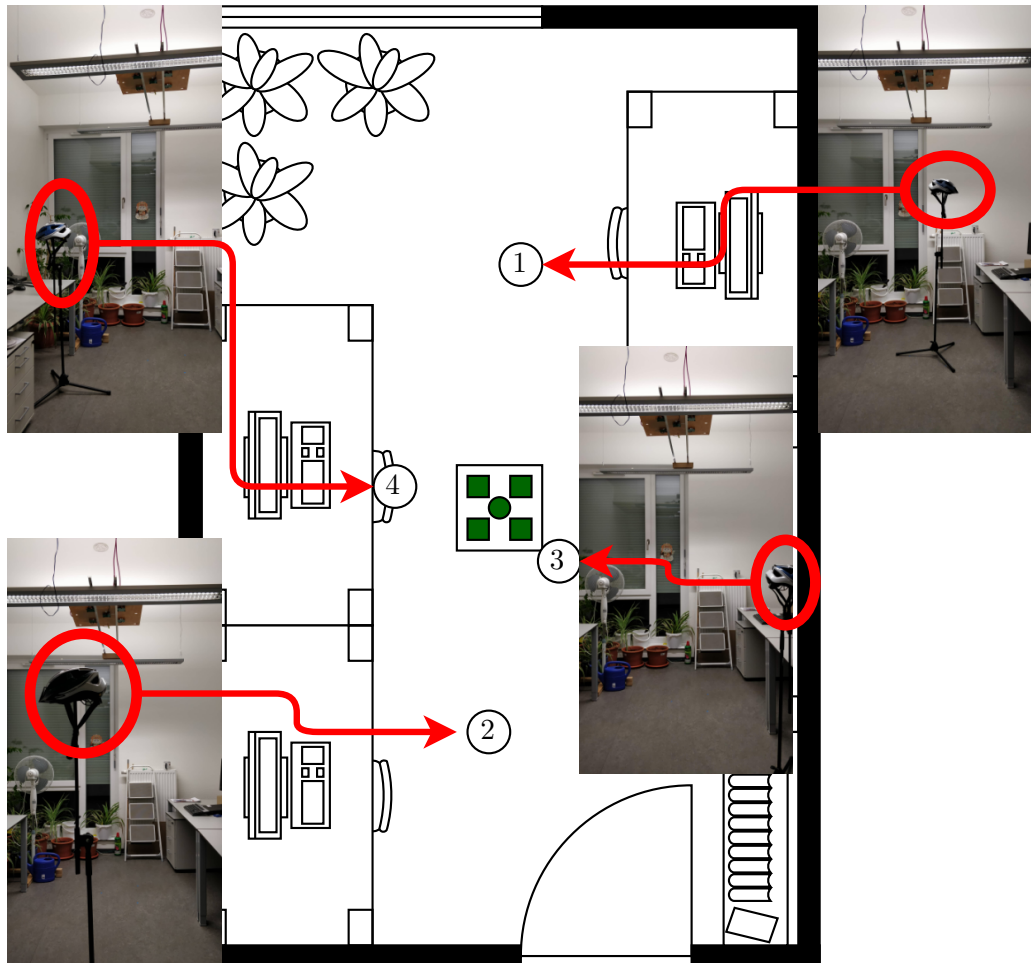


Figure 5.15.: Experiment Setup Static object positions are indicated by numbers in circles.

Figure 5.15 show the object location for each measurement. The distances between

the object and each elements on the device is measured using a laser distance sensor. The measured distances in Table 4.16 are used to calculate the coordinates in Table 5.3 with the equation from Section 4.4. The coordinates are calculated with the center of the device as the reference point. The height of the object in each position is also different. In the first two position, the height of the object is 1.2 m from the ground. In position 3 and 4, the object height is set to 0.8 m. The helmet has an irregular ellipsoid shape, with size of 30 cm long and 25 cm width.

Table 5.2.: Measured Distances

Distances (m)	Speaker	Mic 1	Mic 2	Mic 3	Mic 4
Location 1	1.041	1.105	1.138	0.981	0.950
Location 2	1.077	1.008	1.006	1.308	1.181
Location 3	1.227	1.146	1.244	1.308	1.215
Location 4	1.219	1.298	1.179	1.157	1.276

Table 5.3.: Calculated Coordinates

	Distance (cm)	ϕ (rad)	θ (rad)	x (cm)	y (cm)	z (cm)
Location 1	104.48	1.3497	-0.6654	18.02	80.19	-64.50
Location 2	109.20	4.6830	-0.5541	-2.73	-92.82	-57.46
Location 3	122.82	5.6749	-0.9498	58.64	-40.84	-99.89
Location 4	122.75	2.9588	-0.9209	-73.04	13.50	-97.73

Direct Intersection

The method described in Section 4.4.4 resulted in arrays of points coordinates displayed in Figure 5.16. The mean of the coordinates are shown in Table 5.4, with standard deviation of 6.70 cm and the accuracy of 17.72 cm when compared to calculated distances in Table 5.3.

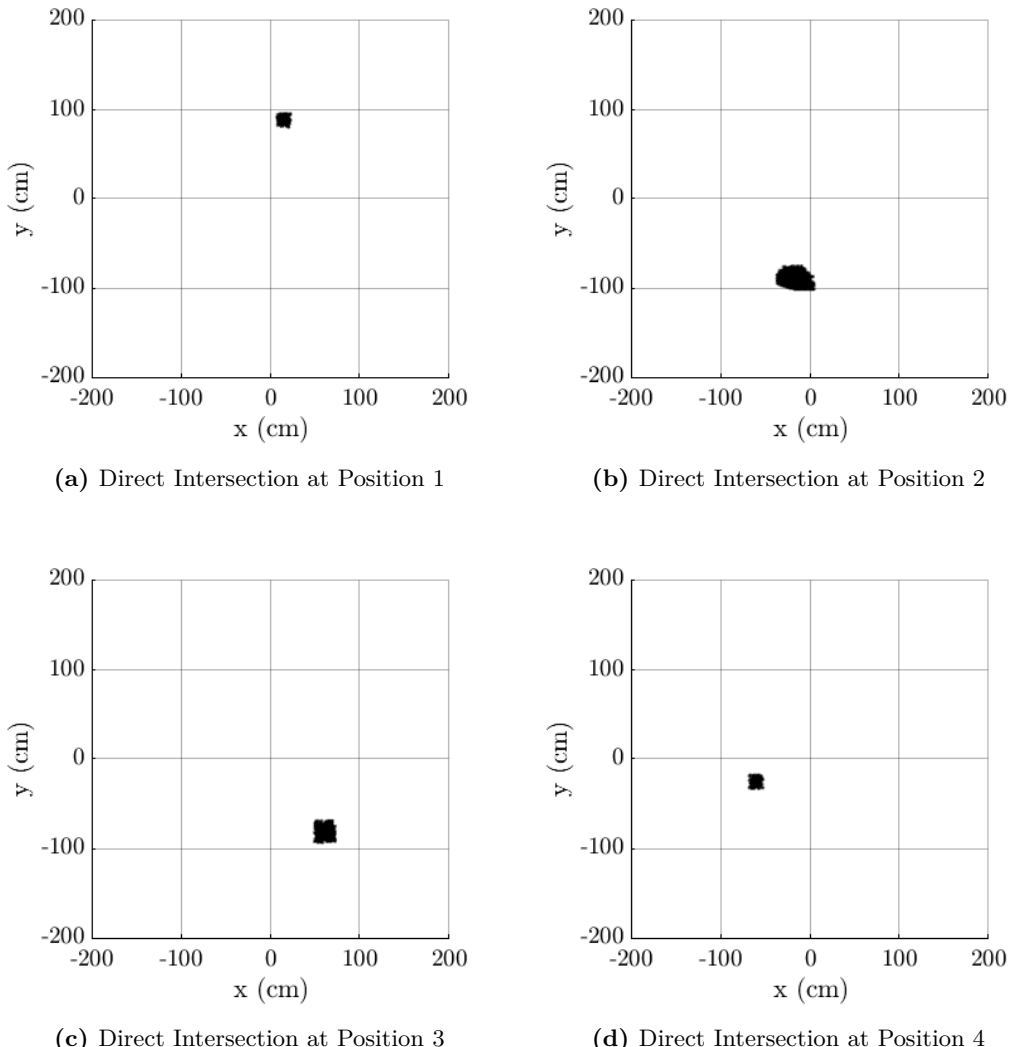


Figure 5.16.: Direct Intersection Results

Table 5.4.: Direct Intersection Coordinates

	x(cm)	y(cm)	z(cm)
Location 1	14.59	89.29	-40.48
Location 2	-17.19	-93.60	-30.43
Location 3	61.81	-81.06	-62.58
Location 4	-60.83	-25.27	-95.55

Sonogram

The sonogram method mentioned in Section 4.4.5 is able to detect objects reliably, however the accuracy highly depend on the correct height of detection. This is essentially the horizontal cut of the direct intersection method, however values that are masked in the previous method can be seen in sonogram. Due to its nature of taking the entire room impulse response, some clutter is also detected at lower heights. The sonogram images from the experiment is displayed in Figure 5.17. Position 1 and position 2 are shown at 1.2 m height, while position 3 and position 4 is at 0.8 m.

Angle of Arrival and Time of Flight

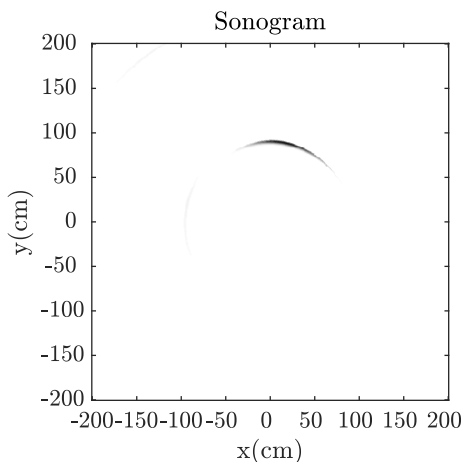
As explained in Section 4.4.6, the spherical coordinates of the detected acoustic wave reflection cane be calculated. By dividing the the incoming wave direction into eight sections and applying equations from Equation (4.12), Equation (4.21), and Equation (4.12). The result of the calculation can be found in Table 5.5. The distance accuracy of this method is 5.22 cm and angular accuracy of 0.9062 rad.

Table 5.5.: AoA and ToF Spherical Coordinates

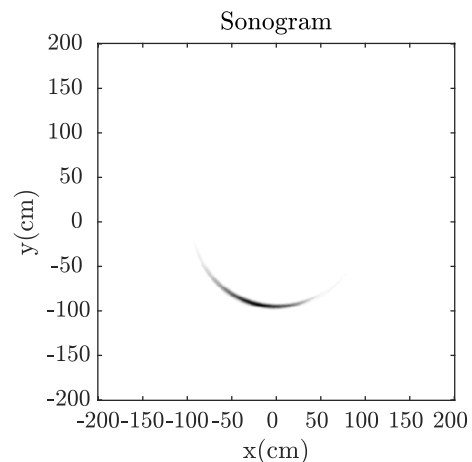
	Distance (cm)	Azimuth (rad)	Elevation (rad)
Location 1	99.13	2.8786	-0.4214
Location 2	102.43	6.0858	-0.3161
Location 3	120.31	0.6435	-0.5600
Location 4	116.50	5.1095	-0.9648

5.4.2. Helmet vs Head Reflection

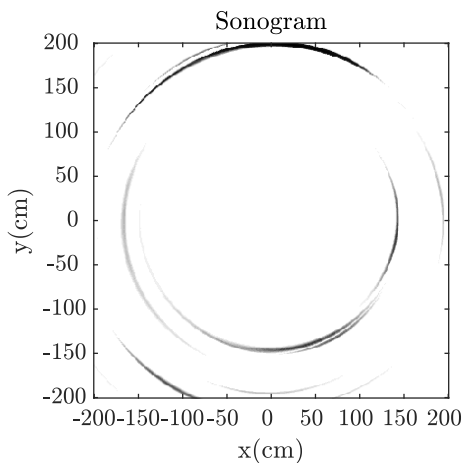
The author compare the addition of helmet to improve acoustic echo presence of a person. Due to lack of available subjects, in the experiment the author sit in



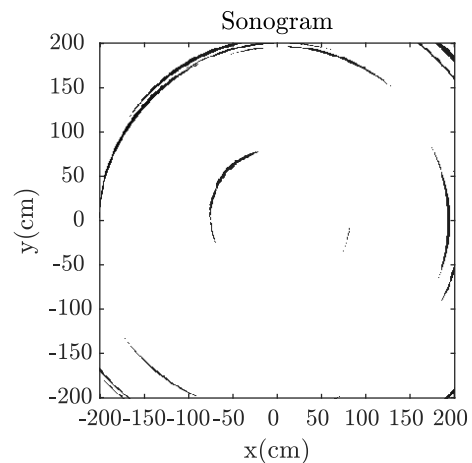
(a) Sonogram of Position 1



(b) Sonogram of Position 2



(c) Sonogram of Position 3



(d) Sonogram of Position 4

Figure 5.17.: Direct Intersection Results

position 3 as illustrated in Figure 5.14. The resultant room echo profiles are shown in Figure 5.18. In all channels, the addition of the helmet seems to greatly improve the

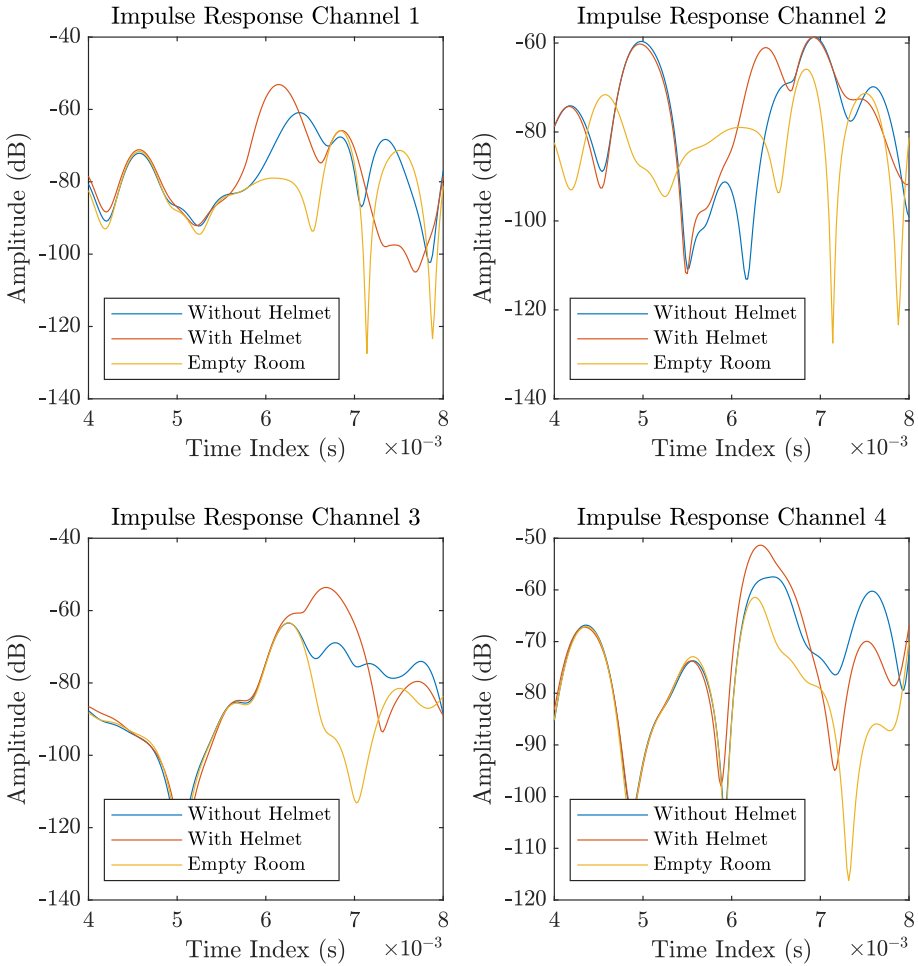
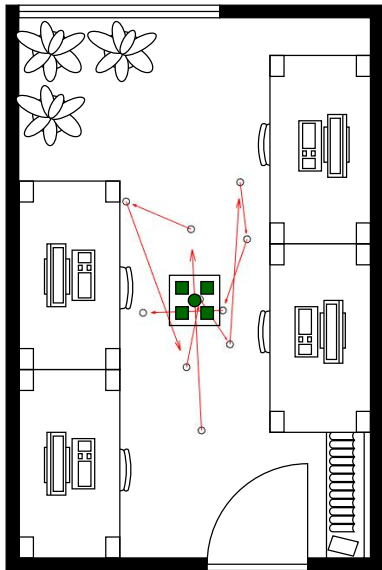
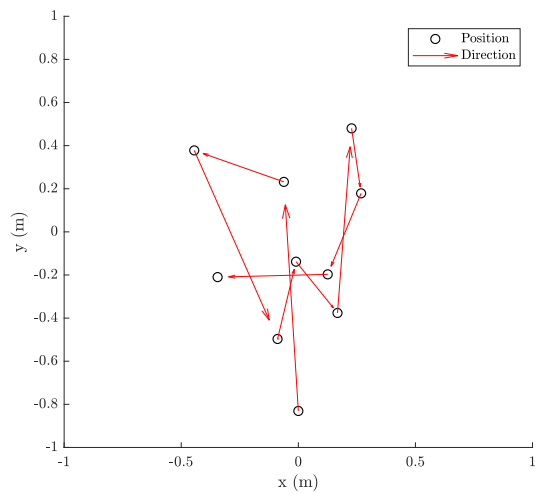


Figure 5.18.: Head vs Helmet

presence of the author. Even though the helmet surface is not smooth, the acoustic reflection of the helmet is still better than without a helmet. As shown in Figure 5.18 an improvement of 5 to 15 dB in all channels due to wearing the helmet.



(a) Movement in the room



(b) Tracking of Movement

Figure 5.19.: Elementary Tracking

5.4.3. Elementary Tracking

Figure 5.19 shows the elementary tracking for a single occupant scenario in an office by consecutive localization of the occupant. The detection time varies between one to five second per location, due to the movement of the occupant. Figure 5.19 (b) shows the movement of a the occupant calculated from method explained in Section 4.4.6 and Section 5.4.1. Figure 5.19 (a) shows the data points from Figure 5.19 (b) overlaid inside the experiment room. The system currently does not consider Doppler effect or any other factors due to target movements, therefore localization is only possible for step changes in position.

6. Discussion and Conclusion

There are some challenges for detecting and locating a presence in a small room by echolocation. This work is intended to build a prototype and to be a foundation work for future development in this research topic. In this chapter we evaluate the hardware and software followed by the conclusion of this work. Additionally, the future outlook and the recommendation for further research is in the last section.

6.1. Hardware Evaluation

6.1.1. Transmitter

The transmitter have a maximum sampling frequency of 44.1 kHz, which means the Nyquist Frequency for the acoustic wave is 22.5 kHz. Moreover since the speaker is working far outside of optimal frequency, an external amplifier is needed to increase the transmitted power. The hardware validation step in Section 5.1 is required to verify that the transmitter chain is able to send out the chirp signal. To have better omni-directionality back of the speaker must not attached to hard surfaces.

6.1.2. Receiver

The receiver chain from microphone, pre-amplifier, active filter and ADC are validated in Section 5.1 as well. The chain is tested with sine sweep or chirp signal to verify

that the whole chain is able to work at the working frequency. While only four microphones is used in this work, the receiver is an eight channels receiver. The ADC has a maximum sampling frequency of 44.1 kHz, with better controller this frequency can be used. The device is designed to be flexible, the control layer can be removed and replaced with better controller. The microphone array is fixed to a acrylic plate to have a well defined distances between elements of the device. Several different arrangement can be set up on to the plate.

6.2. Software Evaluation

6.2.1. Transmitter

The transmitter microcontroller program have to play a well defined sequences. The overhead for sound conversion inside the micro controller can be avoided by translating the sound signal into the sketch, effectively saving the signal sequence into an array in the internal memory. The advantage of using transmitter with microcontroller instead of commercial audio interface is that the external trigger is relatively simple to implement.

6.2.2. Receiver

The receiver microcontroller program control the ADC to sample at defined frequency. For the frame based operation, the microcontroller buffers an entire frame into the ram and then send the data via USB to the computer for further processing. The recording is started when an external trigger is received. Additionally, an error detecting variable is also sent with the data. This variable is a simple sequence of number that indicate the time index of each sample.

6.3. Digital Signal Processing

All the DSP in this work is done in MATLAB for the ease of development. The received echoes are cross-correlated with the reference signal, then the `envelope` function is used to calculate the echo profile. To remove cluttering and unwanted signals from the profile, an empty room profile is used to subtract the target impulse response.

6.4. Localization

Presence detection by methods described in Section 4.4 are used for the experiments in Chapter 5. Each method is able to resolve the position from the reflected acoustic wave, provided the empty room echo profile is available. There are some difficulties in using the static object as the target for the experiment. As one would expect, the reflection points and surface from the object are uncertain. Therefore a certain amount of errors are expected due to irregular and uneven surfaces. Using the direct intersection method from Section 4.4.4, we are able to locate and visualize the reflecting surface. This method is very fast and require light computational resource, however it also require synchronicity between channels to be able to intersect a point.

The sonogram generated from the method described in Section 4.4.5 is used to display the room impulse response from all channels. While it can display and even detect the location quite well, it has some limitation due to the fact that the sonogram work in slices instead of in three dimensions. While we can calculate the three dimensional version, it is very resource intensive to display the result or to derive a location from it.

The angle of arrival and time of flight methods work quite well to derive the spherical coordinates of reflecting objects. As explained in Section 4.4.6, the symmetric

arrangement of microphones is required to use these methods. By dividing the incoming echo direction into eight sections, the azimuth ϕ can be calculated. The elevation θ is calculated by comparing the elapsed times and the distances between microphones perpendicular to the wave front.

Elementary tracking is possible with the current system, however its is done with severe limitation such as low update rate and require a controlled environment. While tracking an object is outside the scope of this work, the author would like to point out this possibility for future development.

6.5. Conclusion

Echolocation is a method of detection used by bats and dolphins in nature, the system developed in this work is based on this principle. Similar to bats, a frequency modulated sine sweep signals or a chirp signals are used as the acoustic signals for echolocation. The system developed in this work is classified as a passive localization system, it is used without tags or sender devices attached to target objects. However it is also classified as an active sensor due to the transmitter sending out acoustic waves for echolocation.

The system construction has several trade-offs due to limited resources. While higher sampling rate is desired, it also means more data need to be processed and transmitted to the computer, which create bottlenecks in the process. The frame based data acquisition is one of the consequences of the trade-offs, after sampling for a period of time the data frame is transmitted to the computer and processed further.

The distances between microphones are the result of several considerations. If the distances is too far, The microphones are placed closer to the walls and received higher amplitude from the walls reflections. Furthermore, if the microphones are

too far apart from the device, the approximation that the object have normal vector pointing to the device is no longer valid. The point of reflections would spread too far apart. If the microphones are placed too close to the center of the device, the device would have reduced the ability to distinguish the timing between impulse responses, effectively reducing the resolution.

The author only consider the linear up-chirp signals in this work. While other signal configurations can be used for echolocation, previous works indicates this type of signals is can be used for localization purpose e.g. distance sensors.

Three different methods to detect and localize presences are explained in Chapter 4 and used in the experiments in Chapter 5. All methods are able to work reasonably well, despite some difficulties regarding inconsistent reflecting surfaces. Elementary tracking by consecutive localization is also possible with some limitations.

The device developed in this work is intended to be a prototype for similar research, the author hope that this work can serve as a foundation work for future development in this topic of interest.

6.6. Future Outlook

Presence detection is an important part for energy managements. To avoid privacy concerns, a passive localization device that does not capture images is highly desired. The system developed in this work can be used gor this purpose. While some can argue that there is a possibility of voice recording, a voice cancelling filter can be directly put into the hardware to reduce the privacy risk. Detecting presence by echolocation, especially in a small room present a challenging but very interesting topic.

6.7. Recommendation for Hardware Development

- To have more bandwidth, a higher frequency acoustic wave is required to avoid audible disturbances. Therefore higher sampling rate as well as faster hardware is needed.
- Larger array of microphones can be used to improve the system performance.
- Specialized signal processing hardware such as DSP chip or using an FPGA to speed up the system and avoid bottleneck.
- Beamforming acoustic transmitter for steerable high directivity acoustic wave transmission.

6.8. Recommendation for Software Development

- Do some parts of DSP on microcontroller level to optimize resource usage.
- Take advantage of parallel byte communication between ADC and Microcontroller.
- Use faster communication protocol between the Microcontroller and the Computer.
- Create an application or a stand alone program for detecting and locating presence.
- Possible integration into ROS ecosystem.

6.9. Recommendation for Localization and Tracking

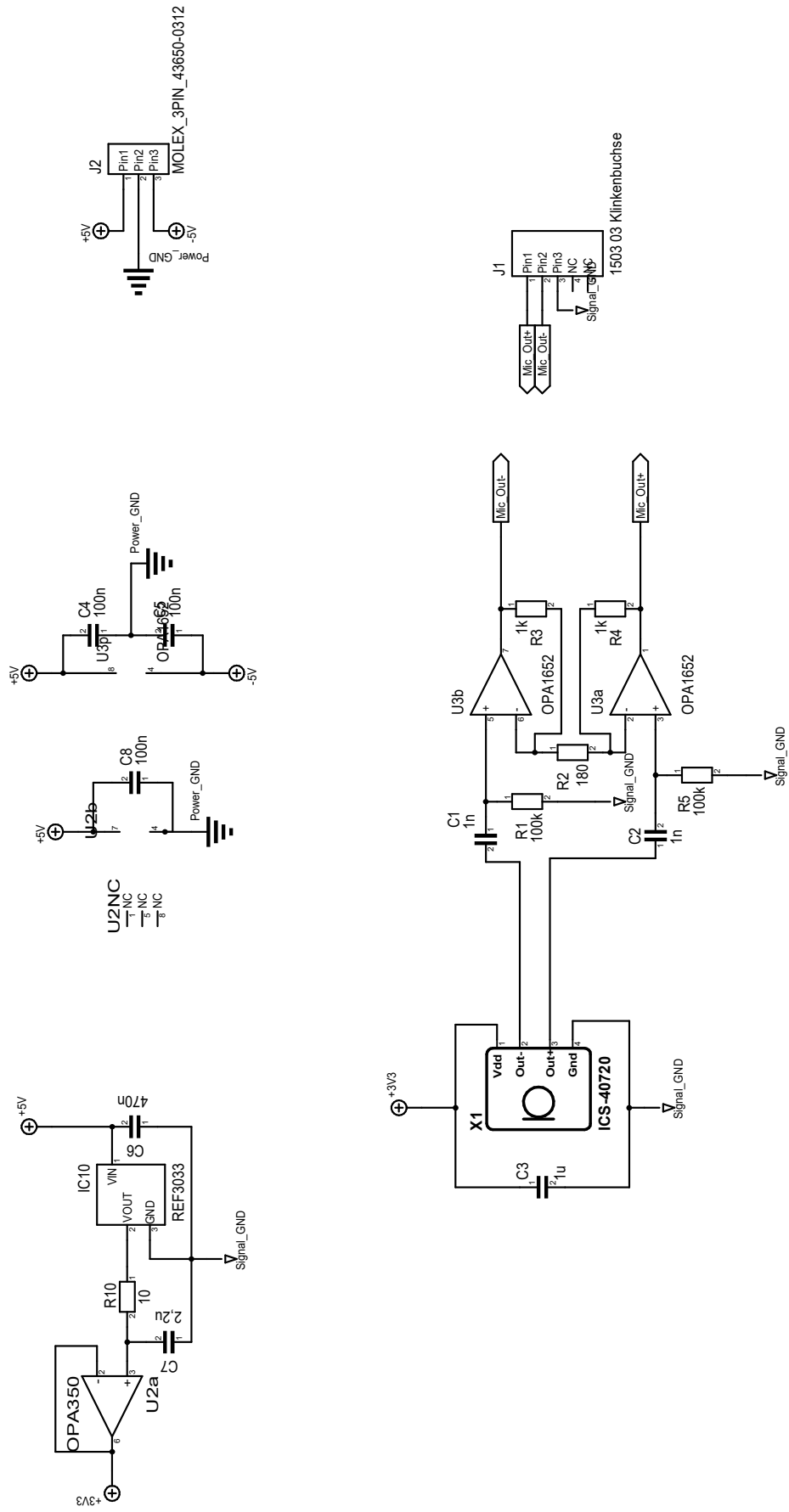
- Consider the Doppler effect and other movement factors.
- Consider the use of Artificial Intelligence to detect and locate presence.

7. Acknowledgments

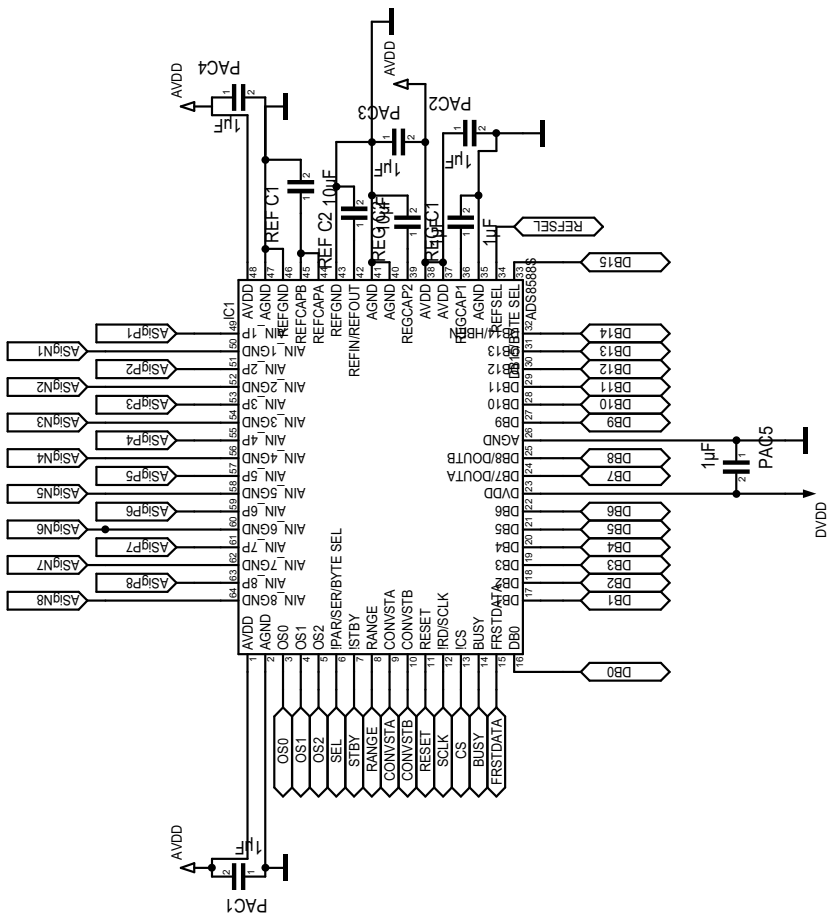
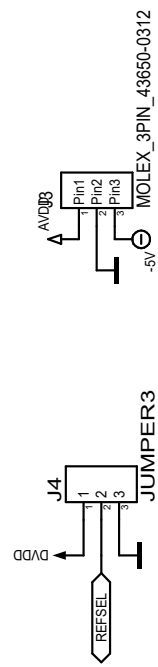
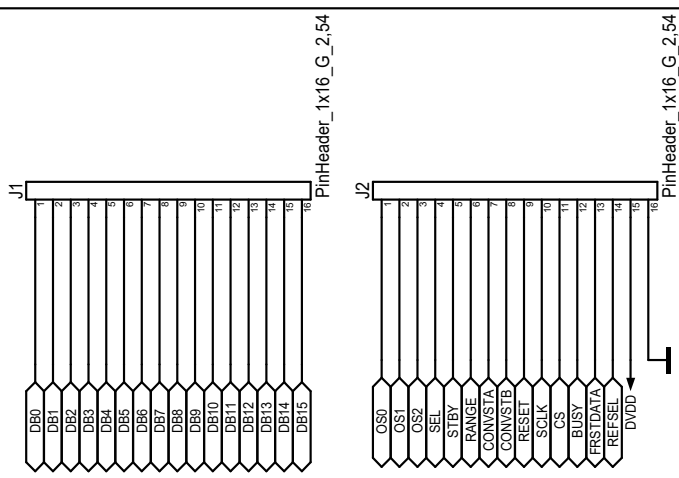
I would like to thank Prof. Reindl and Prof. Schindelhauer as the examiner and co-examiner of this thesis, as well as Dominik Jan Schott as the advisor of this work. I also would like to thank Telocate GmbH and the people that has supported me and providing opportunity to explore this research topic, especially Fabian, Johannes, Joachim, Rui, Sebastian, Andrea and Fisnik who have contributed to this work. I cannot done all of this without support of my family, friends and colleagues, especially Hazal, Muhammad, Mohsin, and others. I would also extend my thanks to Uni-Freiburg and everyone else who has supported me during my study here, including all the Professors, Lecturers and Staffs.

A. Appendix

A.1. Schematics

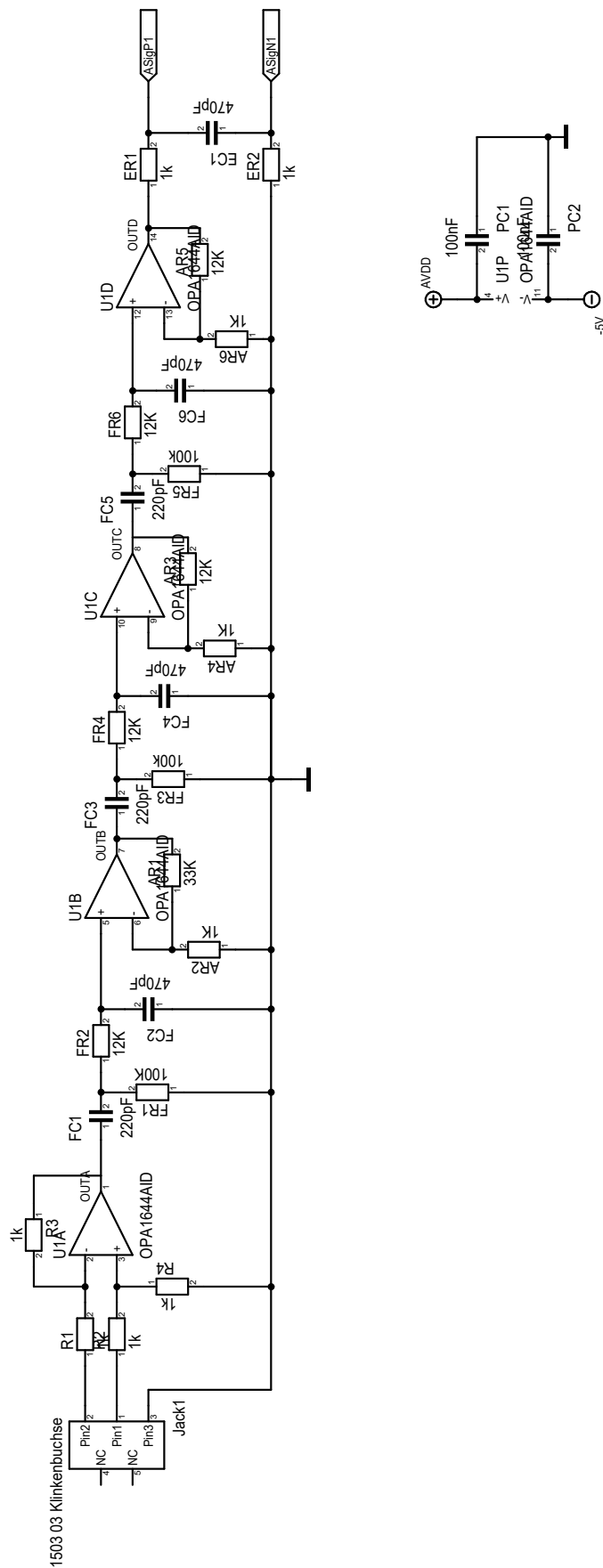


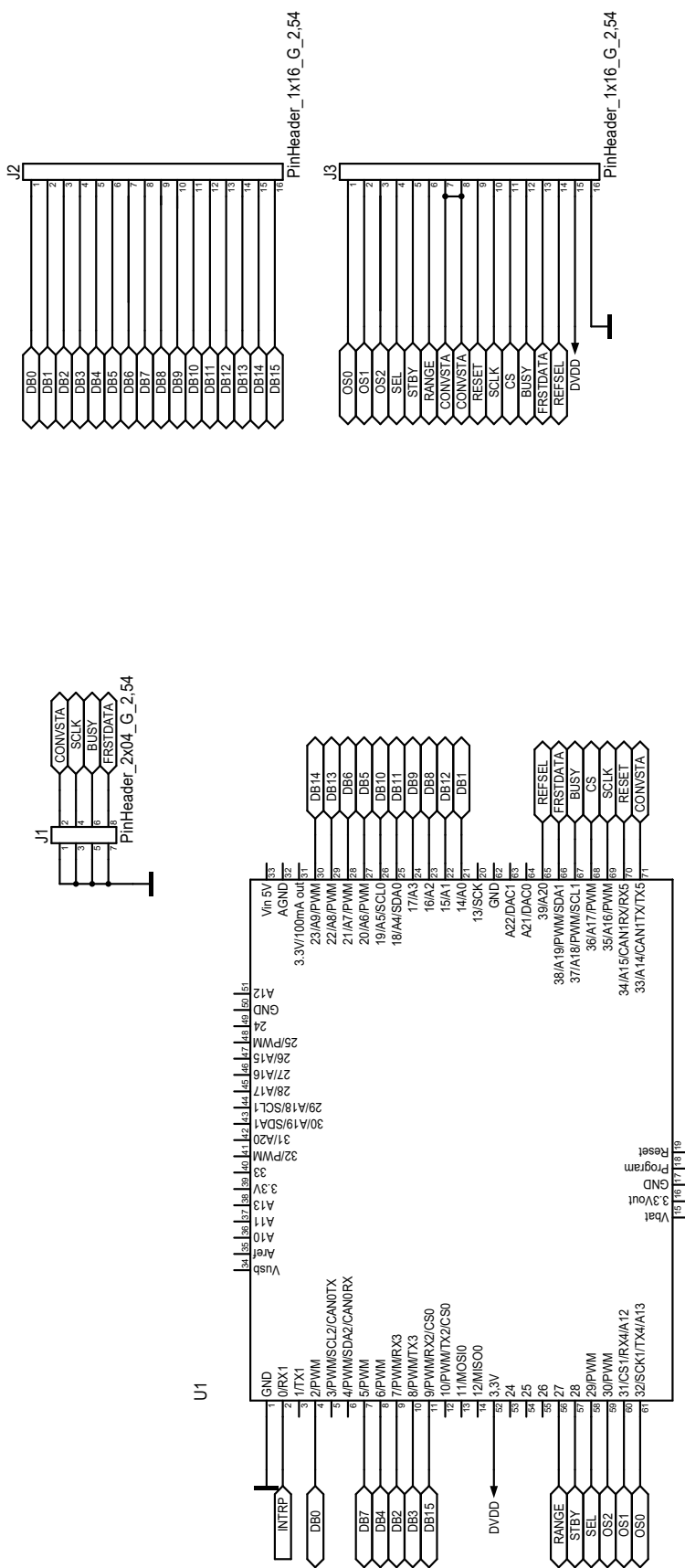
Maßstab	95.14%	Firma	Telocate	Zeichner	A. Saphala	Blatt	1
Änderung	2018-06-06	17:04		Title	Microphone		
Ausgabe	2019-07-24	09:10					
Datei	Microphone-final-20180606.T3001			Projekt	Eight Channels Tranciever		



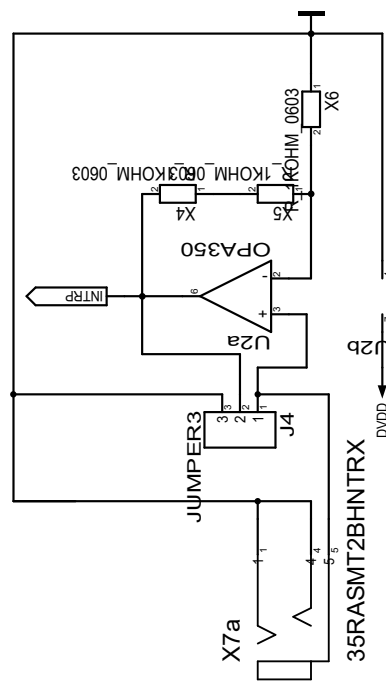
Maßstab	95.14%	Firma	Zeichner	Blatt
Änderung	2018-06-06	13:12		
Ausgabe	2019-07-24	09:16		
Datum	Reciever-final	20180606.T3001	Projekt	

Maßstab	95.14%	Firma	Zeichner	Blatt
Änderung	2018-06-06	13:12	Title	
Ausgabe	2019-07-24	09:16		
Datum	Reciever-final	20180606_T3001	Projekt	

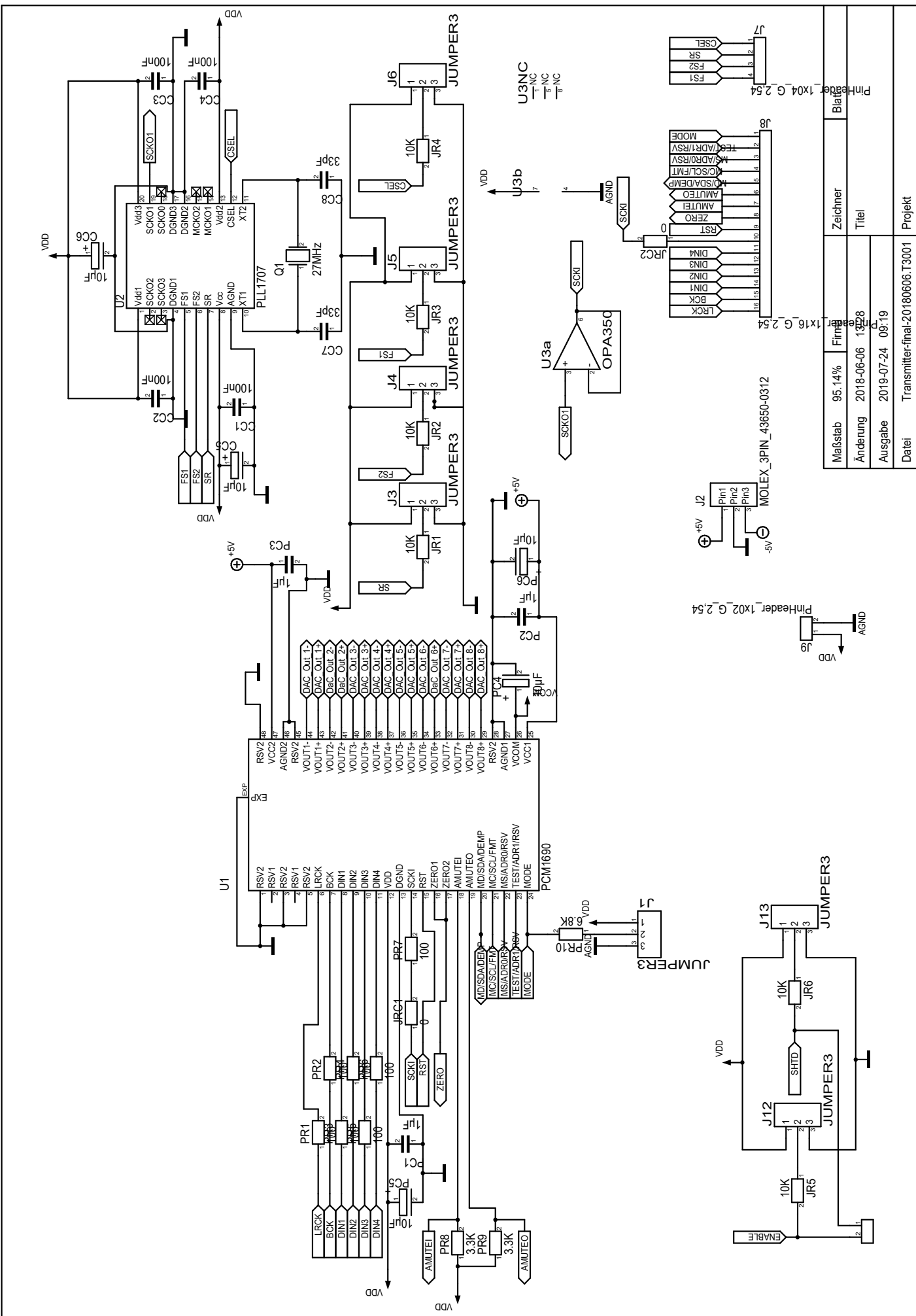


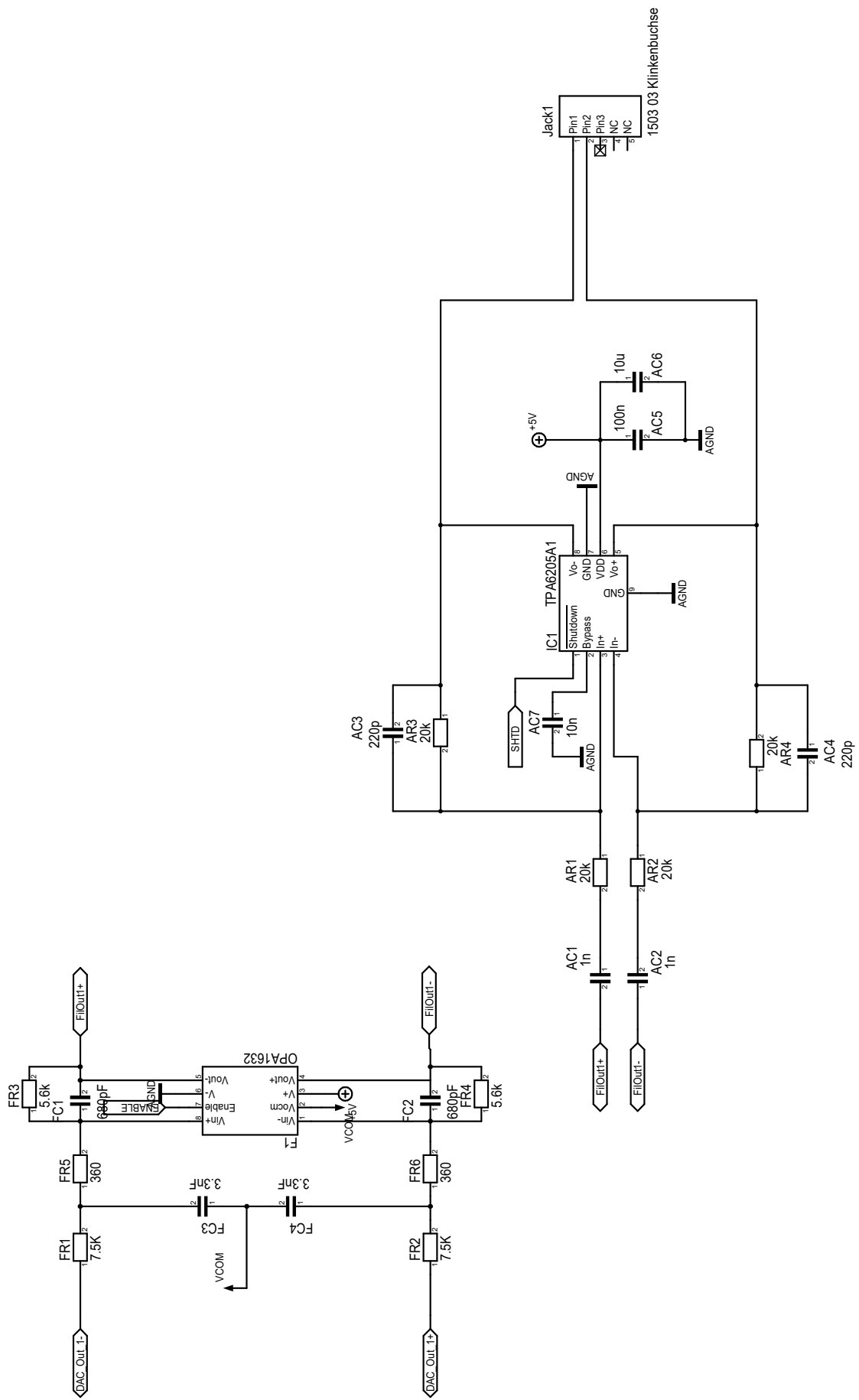


Teensy 3.6



Maßstab	95.14%	Firma	Zeichner	Blatt
Änderung	2018-12-06	15:32		Title
Ausgabe	2019-07-24	09:22		
Daten	Control-V2.5.T3001		Projekt	





Maßstab	95.14%	Firma	Zeichner	Blatt
Änderung	2018-06-06	13:28		Title
Ausgabe	2019-07-24	09:19		
Datum	Transmitter-final-20180606.T3001		Projekt	

Bibliography

- [1] J. Patel and G. Panchal, “An iot-based portable smart meeting space with real-time room occupancy,” in *Intelligent Communication and Computational Technologies* (Y.-C. Hu, S. Tiwari, K. K. Mishra, and M. C. Trivedi, eds.), (Singapore), pp. 35–42, Springer Singapore, 2018.
- [2] H. N. Saha, A. Mandal, and A. Sinha, “Recent trends in the internet of things,” in *Proc. IEEE 7th Annual Computing and Communication Workshop and Conf. (CCWC)*, pp. 1–4, Jan. 2017.
- [3] S. Soumya, M. Chavali, S. Gupta, and N. Rao, “Internet of things based home automation system,” in *Proc. Information Communication Technology (RTEICT) 2016 IEEE Int. Conf. Recent Trends in Electronics*, pp. 848–850, May 2016.
- [4] H. N. Saha, N. Saha, R. Ghosh, and S. Roychoudhury, “Recent trends in implementation of internet of things — a review,” in *Proc. Electronics and Mobile Communication Conf 2016 IEEE 7th Annual Information Technology (IEMCON)*, pp. 1–6, Oct. 2016.
- [5] D. Caicedo and A. Pandharipande, “Distributed ultrasonic zoned presence sensing system,” *IEEE Sensors Journal*, vol. 14, pp. 234–243, Jan. 2014.

- [6] J. C. Chen, K. Yao, and R. E. Hudson, “Acoustic source localization and beamforming: Theory and practice,” *EURASIP Journal on Advances in Signal Processing*, vol. 2003, p. 926837, Mar 2003.
- [7] J. A. Simmons and R. A. Stein, “Acoustic imaging in bat sonar: echolocation signals and the evolution of echolocation,” *Journal of Comparative Physiology*, vol. 135, no. 1, pp. 61–84, 1980.
- [8] L. E. Kinsler, A. R. Frey, and A. B. Coppens, *Fundamentals of Acoustics*. PAPERBACKSHOP UK IMPORT, 1999.
- [9] S. Kentish and M. Ashokkumar, *The Physical and Chemical Effects of Ultrasound*, pp. 1–12. New York, NY: Springer New York, 2011.
- [10] V. Magori, “Ultrasonic sensors in air,” in *Proc. IEEE Ultrasonics Symp. 1994*, vol. 1, pp. 471–481 vol.1, Oct. 1994.
- [11] ITead Studio, *Ultrasonic ranging module : HC-SR04*, Nov. 2010. Rev. 2.
- [12] “LV-MaxSonar®-EZ™ Series High Performance Sonar Range Finder MB1000, MB1010, MB1020, MB1030, MB1040 data sheet.”
- [13] D. Caicedo and A. Pandharipande, “Transmission slot allocation and synchronization protocol for ultrasonic sensor systems,” in *Proc. SENSING AND CONTROL (ICNSC) 2013 10th IEEE INTERNATIONAL CONFERENCE ON NETWORKING*, pp. 288–293, Apr. 2013.
- [14] Toposense, “Faq-toposense.” <https://toposens.com/faq/>. (accessed Jul. 08,2019).
- [15] Toposense, “Ts3-toposense.” <https://toposens.com/ts3/>. (accessed Jul. 08,2019).

- [16] R. Roy, “Ts3 spec sheet.” <https://gitlab.com/toposens/public/resources/blob/master/TS3/ts3-specs.md>. (accessed Jul. 08,2019).
- [17] D. Caicedo and A. Pandharipande, “Ultrasonic array sensor for indoor presence detection,” in *Proc. 20th European Signal Processing Conf. (EUSIPCO) 2012*, pp. 175–179, Aug. 2012.
- [18] D. Caicedo and A. Pandharipande, “Ultrasonic arrays for localized presence sensing,” *IEEE Sensors Journal*, vol. 12, pp. 849–858, May 2012.
- [19] S. Naghibzadeh, A. Pandharipande, D. Caicedo, and G. Leus, “Indoor granular presence sensing with an ultrasonic circular array sensor,” in *Proc. IEEE Int. Symp. Intelligent Control (ISIC)*, pp. 1644–1649, Oct. 2014.
- [20] S. Naghibzadeh, A. Pandharipande, D. Caicedo, and G. Leus, “Indoor granular presence sensing and control messaging with an ultrasonic circular array sensor,” *IEEE Sensors Journal*, vol. 15, pp. 4888–4898, Sept. 2015.
- [21] F. Ribeiro, D. Florencio, D. Ba, and C. Zhang, “Geometrically constrained room modeling with compact microphone arrays,” *and Language Processing IEEE Transactions on Audio, Speech*, vol. 20, pp. 1449–1460, July 2012.
- [22] J. Joyce, “Ultrasonic sensor control system for occupancy sensing,” Sept. 2014. US Patent 8,844,361.
- [23] S. Müller and P. Massarani, “Transfer-function measurement with sweeps,” *Journal of the Audio Engineering Society*, vol. 49, no. 6, pp. 443–471, 2001.
- [24] I. H. Chan, “Swept sine chirps for measuring impulse response [j],” *Power (dBVrms)*, vol. 50, no. 40, p. 30, 2010.
- [25] G. Wahi, A. N. J. Raj, and Zhun Fan, “Swarm bots: System design for echolocation,” in *2017 3rd International Conference on Control, Automation and Robotics (ICCAR)*, pp. 229–232, April 2017.

- [26] B. Cheng, F. Yang, and J. Xu, “A biomimetic model for bats’ echolocation signal processing and it’s implementation on fpga,” in *2010 2nd International Conference on Signal Processing Systems*, vol. 1, pp. V1–452–V1–456, July 2010.
- [27] J. P. Steiner, *Conventional IR and Ultrasonic Sensor Systems*, pp. 1–49. Cham: Springer International Publishing, 2016.
- [28] G. Deak, K. Curran, and J. Condell, “Review: A survey of active and passive indoor localisation systems,” *Computer Communications*, vol. 35, 07 2012.
- [29] “ICS-40720 data sheet,” Jan. 2016. Rev. 1.3.
- [30] “AS01508AO data sheet,” Jan. 2016. Last Revised Sept. 2016.
- [31] F. Zeqiri, “Charakterisierung und Optimierung eines auf Ultraschall basierenden Tags,” b.s. thesis, Albert-Ludwigs-Universität Freiburg, May 2019.
- [32] A. V. Oppenheim and R. W. Schafer, *Discrete-Time Signal Processing*. Upper Saddle River, NJ, USA: Prentice Hall Press, 3rd ed., 2009.
- [33] S. Qureshi, “Cross-correlation and matched filters.” <http://www.drdobbs.com/architecture-and-design/cross-correlation-and-matched-filters/184405317>. (accessed Jul. 23,2019).
- [34] R. Lyons, “How to interpolate in the time-domain by zero-padding in the frequency domain.” <https://dspguru.com/dsp/howtos/how-to-interpolate-in-time-domain-by-zero-padding-in-frequency-domain/>. (accessed Jul. 23,2019).
- [35] I. International, “Fast fourier transform (fft) faq.” <https://dspguru.com/dsp/faqs/fft/>. (accessed Jul. 23,2019).

- [36] WaveMetrics, “Hilbert transform.” <https://www.wavemetrics.com/products/igorpro/dataanalysis/signalprocessing/hilberttransform>. (accessed Jul. 23,2019).
- [37] M. is Fun, “Maxima and minima of functions.” <https://www.mathsisfun.com/algebra/functions-maxima-minima.html>. (accessed Jul. 23,2019).
- [38] Texas Instrument, *ADS 8588s Datasheet*, 12 2016. Rev. April 2017.
- [39] PJRC, “Teensy usb development board.” <https://www.pjrc.com/teensy/index.html>. (accessed Jul. 23,2019).
- [40] Visaton, *AMP 2.2 LN*, 10 2015. available online: http://www.visaton.de/sites/default/files/dd_product/amp2_2ln.pdf (accessed Jul. 23,2019).

